Master's Thesis in Energy

Study specialization: Renewable Energy - Energy Analysis and Optimization

# Wind Farm Layout Optimization

A case study on maximizing the annual energy production in Creyke Beck B.

**Eirin Mæland Fjellanger**

June 2016


Department of Informatics

University of Bergen

**Acknowledgements**

First and foremost I would like to thank my supervisor Professor Dag Haugland, for his great support and guidance. Throughout the project he has provided me with good ideas and useful feedback, which has helped me raise the quality of my work. I would also like to thank him for all the hours he has dedicated to our weekly updates, and the time he has spent proofreading my work.

Next, I would like to thank my supervisor Finn Gunnar Nielsen, who has contributed with valuable input on wind related topics, as well as being a great support in the process of gathering the necessary input data. He has also given me the opportunity of spending some time at Statoil while working on my thesis, which I am particularly grateful for.

I would also like to thank Arne Klein, who has contributed with invaluable technical support related to the installation of the optimization tool TOPFARM. In addition, he has been of great help in the process of getting familiar with the program. In this regard, I would also like to thank Pierre-Elouan Réthoré and Gunner C. Larsen who have assisted me in the process of gaining access to TOPFARM, and been available for TOPFARM related questions throughout the project. Also, I would like to thank Forewind, for allowing me to use their copyrighted picture in my thesis.

Lastly I would like to thank my good friend Maiken Vigsø and my dad Kurt Fjellanger, for proofreading my work, and all my fellow students for five good years at GFI.

**Abstract**

For offshore wind farms, detailed planning, including wind farm design optimization, is becoming increasingly important to secure and increase the wind farm's revenue during its operational life time. Since the energy production represents the wind farm's only economical income, optimizing layouts with the objective of maximizing the annual energy production, can cause a significant increase in profitability for various projects. Motivated by this, the optimization tool TOPFARM, is applied on the planned wind farm Crekye Beck B, to generate optimal layout suggestions with respect to attained annual energy production. TOPFARM is considered a powerful tool for wind farm optimization, but is mainly developed to handle small test cases. Considering the size of the wind farm, the focus in the thesis is thus divided into two parts. The fist part focuses on enabling TOPFARM to run for the required number of turbines, which is handled by developing various implementations. The second part focuses on attaining improved solutions by applying TOPFARM, using three approaches to layout optimization, developed in the thesis. The first approach is constructed to perform optimizations based on three different sets of constraints, for turbine relocation. The second approach is to perform optimizations on various fractions of the available area, and to evaluate the optimal area utilization. The third approach is to optimize the layout by calculating the energy production in the optimization with a higher resolution of included wind speeds and wind directions, than for the other approaches. Based on the results obtained from the various approaches, it is concluded that a further development of TOPFARM is recommended with respect to handling large wind farm cases, in order to attain improved solutions. It is also found, that utilizing only a fraction of the available area might be more profitable, which can reduce expenses with respect to both installation and maintenance.

# Contents

# Chapter 1

# Introduction

The energy market is currently experiencing a continuous growth in demand. Meanwhile, the consumption from the main energy source, fossil fuels, needs to be significantly reduced to prohibit environmentally harmful emissions. This has motivated research and development in new areas, where energy is provided by renewable sources. In Europe for example, a rapid development in different technologies, such as solar and wind, has been an ongoing process. In recent years, the wind industry has also been focusing on new solutions, where energy from wind is harvested offshore.

The main contributor to offshore wind development is Europe, with the United Kingdom (UK) as a leading nation (Ernst and Young (EY), 2015). By 2020, the UK's government has determined that 15 % of their energy will be generated from renewable energy sources (Department of Energy and Climate Change (DECC), 2011). A large amount of this energy is expected to come from offshore wind, which has motivated extensive research and investments in this particular area. Several offshore wind farm projects are already planned, where Dogger Bank, located off the coast of Yorkshire is one of the biggest future projects. The rights to this zone is held by a consortium named Forewind, and they have identified four separate sites within this area, for wind farm development (Forewind, 2016). The planned installation for all the sites combined is 4.8 GW, which by assuming a capacity factor of 0.4, can achieve an annual energy production (AEP) of 16.8 TWh. Given this amount of attained energy, a fully operational Dogger Bank zone can cover

about 5 % of UK's total annual energy consumption (NationMaster, 2011).

Realising a large project like this is not done without difficulties. In order to develop a profitable project, the Levelized Cost of Energy (LCoE), which is dependent on the income from power production versus costs related to installation and operation, needs to be evaluated and minimized. Even though the wind resource is better offshore, costs related to construction are also significantly higher. The installations offshore need to handle a rough environment with powerful storms, wave loads and corrosion. The need for underwater installations also increases the constructional costs, especially regarding foundation and cabling. In addition, by being offshore, stronger wakes are generated, which cause reductions in the attained AEP. To secure and increase the revenue from offshore projects, detailed planning including wind farm design optimization, is becoming an important component in the development of wind farms (Herbert-Acero et al., 2014). The growing interest in the topic, has also motivated the development of several different optimization approaches and optimization tools, constructed to improve the design of wind farms. A promising tool in particular, is the wind farm optimization platform TOPFARM, developed by DTU Wind Energy, which enables an economical wind farm optimization by considering various components (Réthoré et al., 2014).

Since energy production represents the only economical income from a wind farm, optimizing the AEP can have a significant effect on the project's total economical profitability, thus contributing to a reduced LCoE. Motivated by this potential, the scope of the thesis is therefore to minimize the power losses caused by wake effects, for the planned wind farm Creyke Beck B, located in the Dogger Bank zone. In order to attain optimal solutions, the optimization tool, TOPFARM, is used for three approaches considered in the thesis. The first approach aims to improve the design of three initial layouts, inspired by layouts proposed by Forewind (2013a). The second approach challenges the utilization of the available area, and performs optimizations on various fractions of the original area, while the third approach is developed to optimize the layout by calculating the AEP with a higher resolution in velocities and wind directions, in the optimization procedure. Based on these approaches, the thesis aims to attain optimal solutions with the objective of maximizing the AEP, but with an additional evaluation of the optimal layout's profitability.

# Chapter 2

# Background

## 2.1 Extracting energy from wind

The power extracted from wind is the only economical income, therefore good predictions of the energy generation in a wind farm are crucial for a project's financial profitability. The amount of power that can be extracted is dependent on the wind resource at a given location and the turbine performance. To attain valid power predictions, it is thus important to understand the fundamental principles behind the various wind conditions, the individual turbine performance, and the interaction between turbines in a wind farm.

### 2.1.1 Wind resource

A typical feature of the wind conditions is that the wind speed varies with height, usually with an increase in wind speed with altitude. This is because surface friction causes a reduction in wind speed close to the ground. In general, the wind speed $U$ in the surface layer, attains a logarithmic change with height $z$ approximated by

$$U = \frac{u_*}{k} ln \left( \frac{z}{z_0} \right), \tag{2.1}$$

where $u_*$ is the friction velocity, $k = 0.4$ is the von Karman constant, and $z_0$ is the aerodynamic roughness length (Wallace and Hobbs, 2006). The value of the roughness length is dependent on the surface terrain, given by the values in Table 2.1, derived from Table 9.2 in Wallace and Hobbs (2006, p.384). The increase in wind speed with height in the surface layer, is highly dependent on the roughness length. In Table 2.1, it is shown that an open sea generates a short roughness length, indicating low friction between the wind and the surface. As a result, wind profiles over sea areas experience a rapid increase in wind speed with height, thus attaining better conditions for power generation at lower altitudes.

| **Landscape** | $\mathbf{z_0}$ **[m]** |
|---|---|
| City | $\geq 2$ |
| Suburbs | 1.0 |
| Cultivated area | 0.1 |
| Grass prairie | 0.03 |
| Snow-covered fields | 0.005 |
| Sea | 0.0002 |

Table 2.1: Roughness lengths for various landscapes.

Equation (2.1) is based on the assumption that the wind profiles under statically neutral conditions can be represented by a single logarithmic function. Even though the general shape of the wind profile is logarithmic, small variations depending on the atmospheric stability do exist. Stable, neutral and unstable atmospheric conditions appear in all geographical locations, and affect the wind profile at a given site. In Figure 2.1, three typical vertical profiles for a stable, a neutral and an unstable atmosphere, are illustrated with a linear relation between height and wind speed, adapted by Figure 9.17 in Wallace and Hobbs (2006, p.394). Due to an increase in turbulent mixing in an unstable atmosphere, the wind profile in this case experiences a rapid increase, compared to the other cases. However, in a stable atmosphere, the turbulence is too weak to generate a homogeneous surface layer, thus resulting in a delayed wind speed increase with altitude.

The quality of the wind resource is determined by the wind characteristics at a specific site. Since the amount of power that can be extracted from wind is highly dependent on the wind speed, strong and stable winds are more favourable for

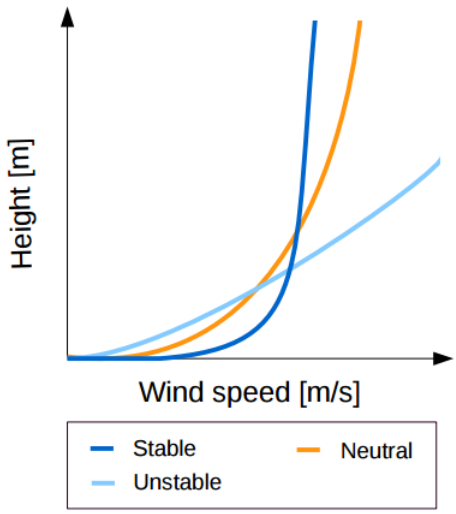


Figure 2.1: Typical wind profiles in a stable, a neutral and an unstable atmosphere.

power generation. In general, the wind resources offshore are superior to onshore sites with respect to power potential. Thus, identifying suitable locations for offshore wind farm development has become a priority within the industry. Figure 2.2, taken from Arent et al. (2012, p.3), provides an overview of the global wind conditions along coastal areas, based on the annual average wind speed at 90 m elevation. The figure shows great offshore potentials in Europe, where most locations are exposed to high average wind speeds.

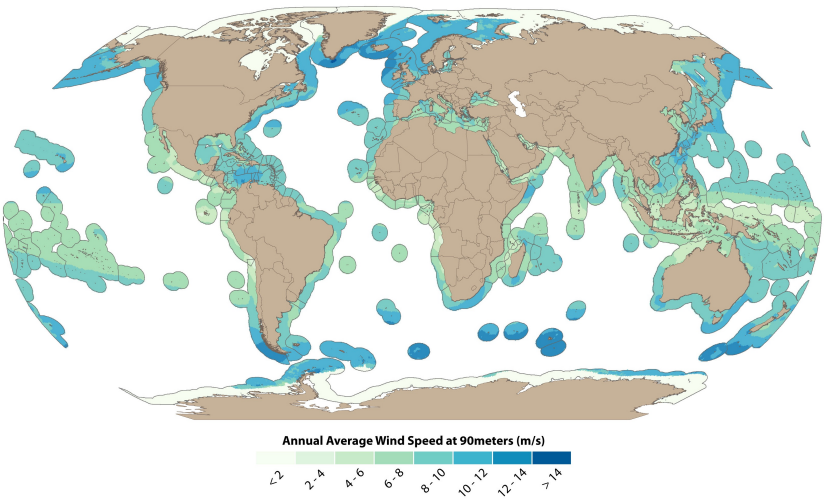


Figure 2.2: Global annual average wind speed map for offshore wind.

### 2.1.2 Power extraction

The amount of power that can be extracted from wind by a turbine, is dependent on the wind conditions and the rotor diameter of the wind turbine, expressed by

$$P = \frac{1}{2} C_p \rho A U^3, \tag{2.2}$$

where P is the power extracted, $\rho$ is the air density, $A$ is the rotor swept area and $U$ is the upstream wind speed. The power coefficient $C_p$ indicates the ratio of the available power extracted by the wind turbine, and is determined by evaluating the difference in wind velocity upstream the turbine, and behind the rotor (Ehrlich, 2013). Using simplified momentum and energy conservation principles, an upper limit of the value of $C_p$ must be derived. From Betz theory, this limit, called the Betz limit, is set to $C_p = 0.593$, resulting in the velocity behind the turbine being one third of the upwind velocity (Okulov and Sørensen, 2008). For real turbines, the value of $C_p$ is not a fixed number, where a typical measure of the value lies between 0.4 and 0.5, for various wind turbines.

The power production attained from a wind resource is dependent on the choice of turbine. Today, several manufacturers producing turbines of various sizes do exist, but the basic structure of the power generation is usually the same. A typical turbine has a cut-in speed, a rated speed and a cut-out speed as shown in Figure 2.3, taken from Løland (2015, p.9). The cut-in speed, which is approximately 3.5 m/s, denotes the required wind speed for power generation. Between the cut-in speed and the rated wind speed, the attained power is increased by approximately the relation given in equation (2.2). The rated wind speed, usually obtained at approximately 12 m/s, defines the limit where the electrical generator reaches full capacity, and maximal power production is attained. To prevent damage to the turbines, the power production is shut down if the wind exceeds the cut-out speed, which is approximately 25 m/s.

The wind turbine's power curve gives an indication of the wind conditions needed to maintain a sufficient power production. It also shows that turbines are sensitive to changes between the cut-in and the rated wind speed.

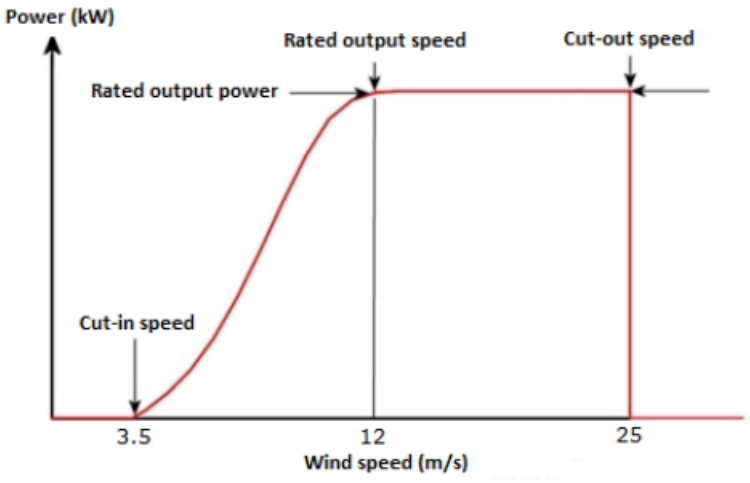


Figure 2.3: A typical power curve for a wind turbine.

## 2.2 Dogger Bank

The Dogger Bank area which is licenced to Forewind for wind farm development, is located between approximately 125 and 290 km off the coast of Yorkshire, in the southern part of the North Sea. Extending over approximately 8660 km$^2$, the area has good prospects for development of several wind farms. The Dogger Bank area is chosen for wind farm development, as the location serves conditions favorable to wind energy production. The area is identified by strong and enduring winds, which are important to maintain a sufficient energy production. In addition, the location is subject to a shallow bathymetry ranging between the water depths of 18 m and 63 m, which is crucial for the wind farm's profitability, considering foundation and installation costs (Forewind, 2013a).

In total, four separate wind farm sites are identified within the Dogger Bank area for future wind farm development. Figure 2.4, taken from Forewind (2012), provides an overview of these sites. A more detailed description of the area and the planned installations is provided in the following sections, with a particular focus on the wind farm Creyke Beck B.

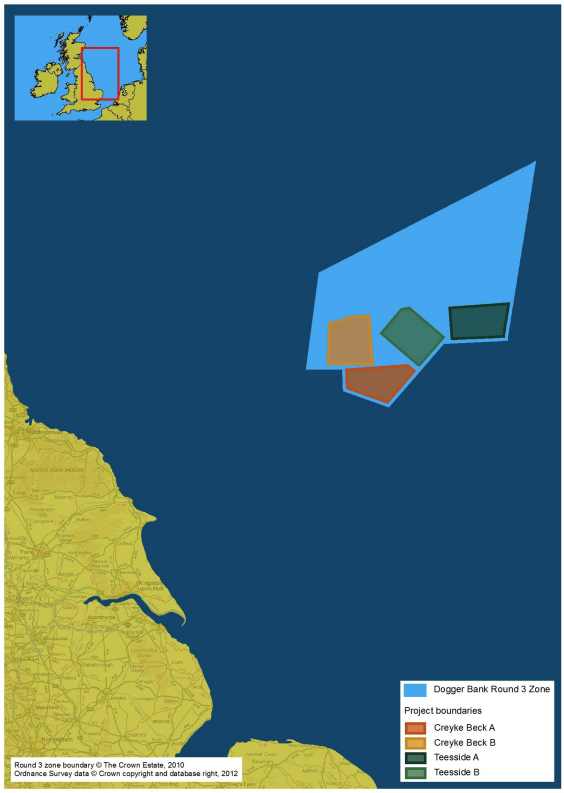


Figure 2.4: The planned wind farms in the Dogger Bank area, map courtesy of Forewind.

### 2.2.1 Site description

The four identified wind farm sites are divided into two different stages of development, named Creyke Beck and Teesside, where a description of each site is given in Table 2.2. The first stage of development, Creyke Beck, includes the construction of the two wind farms located closest to shore in Figure 2.4. These wind farms, named Creyke Beck A and Creyke Beck B, extend over the areas 515 km$^2$ and 599 km$^2$, respectively, with water depths ranging between 20 m and 35 m (Forewind, 2013a). The second stage of development, Teesside, includes the construction of the two remaining wind farms in Figure 2.4, named Teesside A and Teesside B. These wind farms extend over the areas 560 km$^2$ and 593 km$^2$, with water depths ranging between 20 m and 40 m, respectively (Forewind, 2013b). The planned capacity of each wind farm is 1200 MW, which will provide a significant contribution to the British energy market when the wind farms are fully operational.

| | | Creyke Beck A | Creyke Beck B | Teesside A | Teesside B |
|---|---|---|---|---|---|
| **Granted consent** | [y] | 2015 | 2015 | 2015 | 2015 |
| **Area** | [km $^2$] | 515 | 599 | 560 | 593 |
| **Min dist to shore** | [km] | 131 | 131 | 196 | 165 |
| **Water depths** | [m] | 20-35 | 20-35 | 20-35 | 20-40 |
| **Planned capacity** | [MW] | 1200 | 1200 | 1200 | 1200 |

Table 2.2: Information on the planned wind farms in the Dogger Bank area.

### 2.2.2 Planned installation

An operational wind farm which generates and transports electricity to the grid, is dependent on several key components. In addition to energy production from the wind turbines, components handling the electricity are needed, to maintain a safe and efficient energy distribution to market. For the planned wind farm Creyke Beck B, key components to be installed are

- Wind turbines
- Collector stations
- A converter station
- Meteorological masts
- Cables

The number of installed wind turbines is highly dependent on the turbine size. The turbine type to be used in Creyke Beck B is not yet specified, which leaves the number of installed turbines uncertain. In the report by Forewind (2013a), several turbine sizes are suggested, ranging between 4 MW and 10 MW. Considering that the planned capacity for each site is set to 1200 MW, the number of turbines installed can thus range between 300 and 120 turbines, where the two extremes are attained by choosing 4 MW and 10 MW turbines, respectively.

In order to gather the generated electricity from each wind turbine, the installation of several collector platforms is needed. The collector platforms are offshore structures designed to receive electricity from individual wind turbines, and to increase the power voltage with a transformer. In this way, the electricity from various turbines is collected and transmitted in a more efficient manner. Since the distance to shore is relatively long, a converter platform is also needed. The converter platform transforms the electricity from High Voltage Alternating Currents (HVAC) to High Voltage Direct Currents (HVDC), which are more efficient for long distance electricity transports. Apart from the installations related to production and electricity transfer, meteorological masts are also installed to measure the wind conditions. An overview of the components and their connections within the wind farm is provided in Figure 2.5.

The installation of cables is necessary to connect all the components together. Forewind (2013a) states that the cabling system should consist of four different cable types. Inter array cabling connecting the wind turbines to the collector platform, and inter platform cabling connecting the converter platform to the collector platform, are two of the cable types suggested. In addition, HVDC cables for electricity export to shore, and inter platform cables which are either HVAC or HVDC, are proposed.

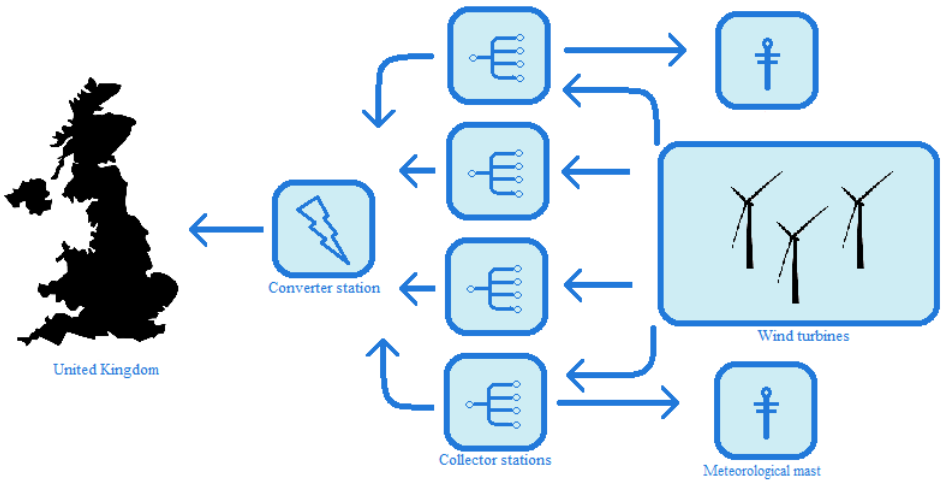


Figure 2.5: Overview of the components and their connections in Creyke Beck B.

### 2.2.3 Regulations and rules

The design of the wind farm layout is highly important, as this has a significant influence on the profitability of the project. Preferably, the wind farm layout is decided with the objective of minimizing the LCoE. In practice however, the layout also needs to fulfill certain rules, even if the result is a less optimal layout. The rules are constructed for several reasons like safety, environmental impact or ship traffic, and are derived from either international standards or from site specific decisions. In this section, some of the layout rules which apply to Creyke Beck B are addressed. The rules are obtained from the report by Forewind (2013a), and are related to restrictions for the turbine placement.

**Layout patterns**

The wind turbine layout, including the additional installed components, is to be organized in a pattern, as either straight or curved lines with a maximum deviation of ±150 m, as far as practically possible. The flexibility of ±150 m for the positioning of turbines, is included to enable micro-siting with respect to components such as sea bed conditions, water depth, or dominant wake conditions. By maintaining this rule, safe navigation within the wind farm is accomplished.

**Boundary conditions**

The boundaries of two opposing wind farms which are closer than 5 km to each other, need to be designed so that they are parallel to one another. In addition, the boundaries are to be marked, so that the two separate wind farms are easily distinguished. All installed components must also be located fully within the boundaries of the site, including the rotor swept area of the wind turbines.

**Wind turbine spacing**

The wind turbine spacing is dependent on the size of the wind turbines. As the turbine size grows, the wake region behind the turbine increases. Thus, for larger turbines, the spacing between them must be increased. The minimum acceptable turbine distance center to center, is defined by Forewind (2013a) as the largest of the two values 700 m and 6D, where D denotes the rotor diameter of a turbine.

**Existing infrastructure**

Existing infrastructure, such as pipelines and cables, needs to be taken into account

when planning the layout. Space is to be left open, so that the existing components can be accessed without difficulties, for maintenance issues. In Table 5.2 in the report by Forewind (2013a, p. 180), the minimum acceptable separation distances to existing infrastructure are displayed.

### 2.2.4 Power potential

The wind resource of Creyke Beck B is analyzed using Nora10 data, which will be described in further detail in Section 3.2.2. The data represent the wind conditions at 119 m elevation, where the distribution of the wind speeds is presented in Figure 2.6, arranged into bins of 1 m/s width. The average wind speed is estimated to 10.1 m/s, which indicates a good potential. In addition, the frequency of the wind speeds observed within the range of 4 m/s and 25 m/s, is approximately 0.92.

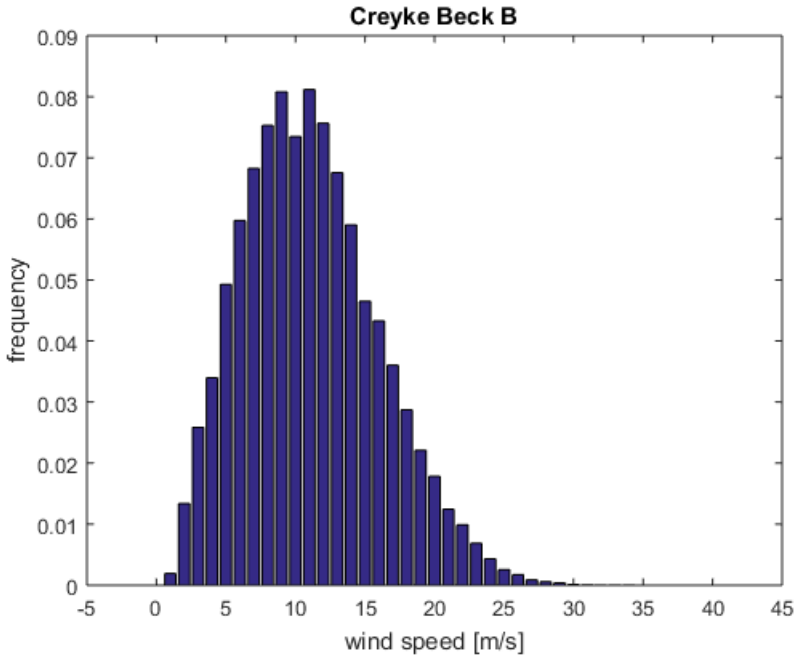


Figure 2.6: Wind speed frequency distribution at 119 m elevation

A wind rose, displaying the contributions from different wind directions in Creyke Beck B at 119 m elevation, is presented in Figure 2.7. The plot shows that the dominant wind directions are west south-westerly, and that stronger winds are also observed in these directions.

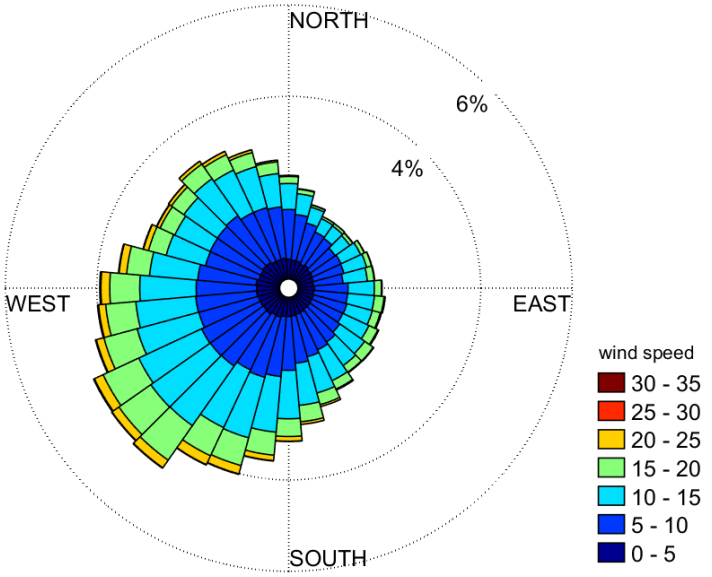


Figure 2.7: Wind rose of Creyke Beck B at 119 m elevation, displaying directional bins of 10 degrees.

In order to obtain power estimates for Creyke Beck B, a 10 MW turbine developed by the Technical University of Denmark (DTU) is chosen as reference turbine in the thesis (see Section 3.2.1). Based on the turbine performance shown in Figure 3.2 and the wind speed frequency distribution in Figure 2.6, the annual power generated by each individual wind speed for a single turbine is found and displayed in Figure 2.8. The figure shows that slightly more power is attained by stronger winds despite their less frequent occurrence, due to the wind turbine performance curve.

Given a 10 MW reference turbine, the total number of installed turbines at Creyke Beck B will be 120. By summing up the annual attained energy from each wind speed in Figure 2.8, and multiplying with the total number of turbines, the annual power output for the wind farm is 5909935 MWh. This corresponds to a capacity factor of 0.562, which is very high. In reality however, it is likely that the capacity factor is lower, as the availability of each turbine in an operating wind farm is less

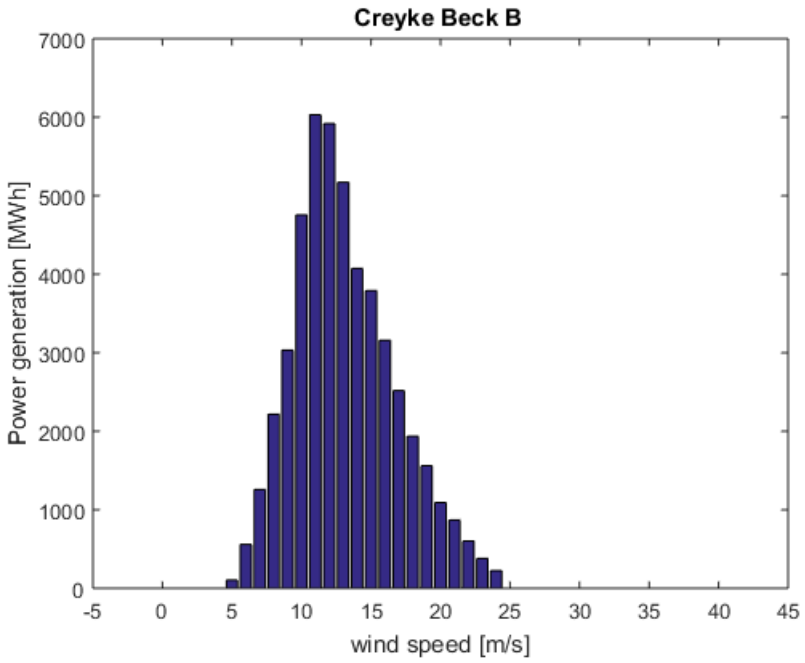


Figure 2.8: Annual generated power per wind speed at 119m elevation.

than 100% (Van Bussel and Zaayer, 2001). Also, wake effects need to be taken into account, which will reduce the capacity factor even further. To provide more accurate power estimations, a further evaluation of the energy losses from wakes is needed.

## 2.3 Wake models

When energy is extracted from air flowing through a wind turbine, the properties of the air flow are changed. In addition to a decrease in wind speed, the turbulence intensity of the air behind the rotor is increased. This change is referred to as the wake effect, and the area behind the turbine affected by this change is called the wake region (Renkema, 2007).

Wakes reaching downwind turbines weaken the wind potential and therefore cause power losses. For large offshore wind farms, it is estimated that between 10 % and 20 % of the total power output is lost due to wind turbine wakes (Barthelmie et al., 2009). The wake loss is greater for wind speeds ranging between a turbine's the cut-in and rated wind speed, as the turbine's performance in this range is highly

affected by wind speed reductions. In addition, wakes endure fatigue loads, which lead to an increase in Operation and Maintenance (O&M) costs, and significantly reduce the lifespan of the wind turbines. Optimizing the location of turbines within a wind farm with respect to wake, is therefore the most important factor to reduce power losses throughout the wind farm's operational lifetime. This has motivated research on the challenging topic of turbulence and wake modelling, to improve the prediction of wakes and their impact on the downstream turbines (Herbert-Acero et al., 2014).

The wake behind a wind turbine can be separated into two sections, namely the near wake region and the far wake region. The transition between these is gradual, and there are several different suggestions to the length extent of the two. Herbert-Acero et al. (2014) state that the far wake region often is considered to start at a distance between 3D and 4D downstream from a given wind turbine. Formally, this distance is based on the length-extent of the wake, which depends on local atmospheric conditions. The models describing the near wake region need to consider several turbulence parameters. This is computationally demanding, and when focusing on entire wind farms, these computations are too expensive. In addition, the spacing of the turbines in a wind farm is usually greater than the extent of the near wake region. Therefore, the wake models used in wind farm optimization usually describe the far wake region (Renkema, 2007).

Different types of modeling approaches are developed to describe the far wake region, ranging from models based on Computational Fluid Dynamics (CFD) to Engineering Wake Models (EWM). The CFD models are advanced wake models, based on Reynolds-Averaged Navier-Stokes (RANS) equations or Large Eddy Simulations (LES). They are considered as powerful tools for simulating the complex wind field in a wind farm, but are computationally expensive to run. The need of less expensive wake models, has therefore lead to the development of simplified CFD wake models. See, for instance, Heggelund et al. (2015), or the description of the linearized CFD model Fuga, in Section 2.5.1. The aim of the simplified CFD models is to maintain a sufficient description of the wake field, but being less expensive to run compared to the original CFD models, due to model reductions or model simplifications.

In addition to the original and simplified CFD models, a variety of EWMs are

developed to estimate wakes. These models describe the wake evolution process in a simplified way, and are computationally inexpensive to solve (Herbert-Acero et al., 2014). A brief description of some of the well known EWMs are provided in the following section.

### 2.3.1 Engineering wake models

In the following, we let $(x, r)$ denote the coordinates of the position in downstream horizontal distance $x$ and radial distance $r$ from the rotor center of a wind turbine. Below, we consider wind speed and wind speed deficits as functions of $x$ and $r$. Whenever there is no variation in the radial direction, we omit the dependency on $r$.

The basic mathematical structure of a EWM can be expressed by

$$U_W(x, r) = U_\infty(1 - U_{Def}(x, r)),$$

where $U_W(x, r)$ is the horizontal wind speed in the wake, $U_{Def}(x, r)$ is the horizontal velocity deficit, and $U_\infty$ is the free stream wind velocity. The EWMs are assumed to provide an acceptable description of the wind speed deficit in the far wake region, but have a tendency to over-predict wake effects. The main difference between these models is usually the way $U_{Def}(x, r)$ is approximated (Herbert-Acero et al., 2014).

#### Jensen model

The simple wake model proposed by Jensen (1983), describes the far wake region behind a single wind turbine. In his model, Jensen assumes the wake to be a negative jet, and the wake expansion to be linear. In addition, the ambient inflow velocity $U_\infty$, is assumed uniform. Thus, the wake radius $R_W^J(x)$ is expressed by

$$R_W^J(x) = \delta x + R_0, \tag{2.3}$$

where $R_0$ represents the initial wake radius, and $\delta$ is an expansion constant. As seen in equation (2.3), the growth rate of $R_W^J(x)$ is dependent on the expansion constant $\delta$, which differs from onshore to offshore cases. Renkema (2007) suggests

that this constant is $\delta = 0.075$ for onshore cases, and $\delta = 0.04$ for offshore cases. A graphical description of the wake generation behind a single turbine, is provided in Figure 2.9.

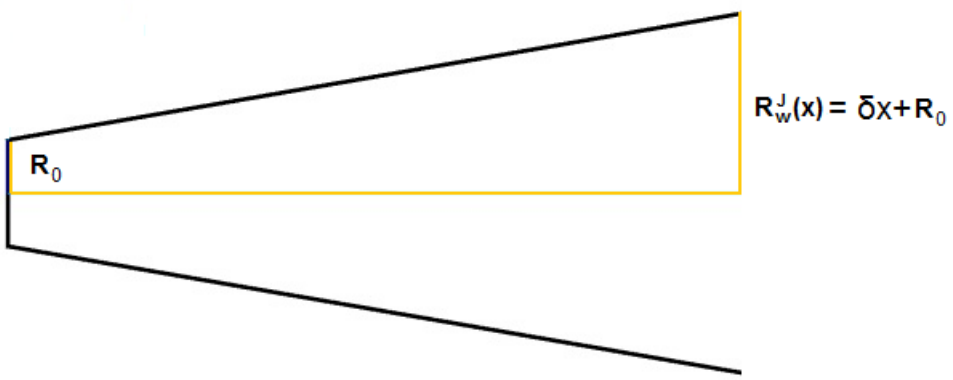


Figure 2.9: Linear wake expansion for a single wake.

The Jensen model includes mass conservation. Therefore, a balanced momentum equation can be generated from the linear wake expansion in equation (2.3)

$$R_0^2 U_0 + (R_W^J(x)^2 - R_0^2)U_\infty = R_W^J(x)^2 U_W^J(x), \tag{2.4}$$

where $U_0$ is the initial wake velocity behind the turbine, and $U_W^J(x)$ is the horizontal wake velocity, only dependent on the downwind distance $x$. Assuming an optimal rotor where the maximum available power is attained, the initial wake velocity is set to $U_0 = \frac{1}{3}U_\infty$ (see Section 2.1.2)(Haugland and Haugland, 2012). Equation (2.4) can then be solved with respect to $U_W^J(x)$, as follows

$$U_W^J(x) = U_\infty \left(1 - \frac{2}{3}\left(\frac{R_0}{R_0 + \delta x}\right)^2\right). \tag{2.5}$$

The Jensen model is a simple and well-known wake model, which in the literature is often applied in wind farm optimization procedures, where the objective is to attain maximum production.

### Katić *et. al*'s wake model

The combination of Katić *et. al*'s and Jensen's wake model, is the most applied wake model for wind farm design optimization problems, according to Herbert-Acero et al. (2014). Based on Jensen's characterization of a single wake from equation (2.5), the horizontal wake velocity $U_W^K(x)$ in the model proposed by Katić et al. (1986) is defined as

$$U_W^K(x) = U_\infty \left(1 - 2e\left(\frac{R_0}{R_0 + \delta x}\right)^2\right),$$

where $e$, the initial velocity deficit, is expressed as

$$e = \frac{(1 - \sqrt{1 - C_T})}{2},$$

where $C_T$ denotes the turbine's thrust coefficient. The thrust coefficient, which is non dimensional, characterizes the thrust or force applied by a specific turbine on the wind, and varies for different values of $U_\infty$. Thus, Katić *et. al*'s wake model differs from Jensen's model, as the calculation of the horizontal wake velocity is dependent on specific turbine characteristics.

The main purpose of Katić *et. al*'s wake model, is to describe the wake effect from multiple turbines, where the single-wake theory is used to develop a model for interacting wakes. In their model, Katić et al. (1986) assume the kinetic energy deficit $U_{Def}^K(x)$ from a mixed wake, to be equal to the sum of the energy deficits from $M$ individual contributing wakes. That is

$$U_{Def}^K(x)^2 = \sum_{n=1}^{M} U_{Def,n}^K(x)^2, \tag{2.6}$$

with the velocity deficit defined as

$$U_{Def}^K(x) = 1 - \frac{U_W^K(x)}{U_\infty}.$$

Equation (2.6) can also be written as an expression for the mixed wake velocity, given by

$$U_W^K(x) = U_\infty \left(1 - \sqrt{\sum_{n=1}^{M} U_{Def,n}^K(x)^2}\right).$$

In later years, Katić *et. al*'s wake model has been implemented in different software programs to estimate the effect from wakes. The Wind Atlas analysis and application Program (WAsP), which is considered a standard software for wind resource assessment, uses the method sescribed in Katić et al. (1986) to model wake effects (DTU Wind Energy, 2016). Further, several programs designed for wind farm optimization, such as GH Windfarmer and WindPRO, use WAsP to calculate the wind farm production (Herbert-Acero et al., 2014).

### Larsen model

In 1988, Larsen (1988) developed a wake model known as the Larsen model, which he later updated in 2009 (Larsen, 2009). The Larsen model is based on the *thin shear layer approximation* of the Navier-Stokes (NS) equations, and includes two versions of different sophistication. The first version which includes first order solutions, only evaluates the dominant terms in the equations, while the second version which also includes second order solutions, takes the full system into account.

In order to obtain solutions for the wake radius and the mean horizontal wake deficit, Larsen assumes an incompressible and stationary flow. In addition, the wind shear is neglected, to enable an expression of the NS equations in cylindrical coordinates. Also, the order of magnitude for each component in the equations is analysed, to further simplify the problem. As a result, first order solutions for the wake radius $R_W^L(x)$ and the horizontal wake deficit $U_{Def}^L(x,r)$ are expressed as

$$R_w^L(x) = \left(\frac{35}{2\pi}\right)^{\frac{1}{5}} (3c_1^2)^{\frac{1}{5}} (C_T A x)^{\frac{1}{3}}, \tag{2.7}$$

$$U_{Def}^L(x,r) = -\frac{U_\infty}{9}(C_T A x^{-2})^{\frac{1}{3}} \left[ r^{\frac{3}{2}} (3c_1^2 C_T A x)^{-\frac{1}{2}} - \left(\frac{35}{2\pi}\right)^{\frac{3}{10}} (3c_1^2)^{-\frac{1}{5}} \right]^2, \tag{2.8}$$

where $c_1$ is a parameter defined in Larsen (1988).

### 2.3.2 A simple stationary semi-analytical wake model

The simple stationary semi-analytical wake model is included in the wind farm optimization software TOPFARM (see Section 2.6), and is constructed to provide a stationary description of the wind field in a wind farm. In the model, wakes are considered as linear perturbations on a non-uniform mean wind field, which allows a linear superposition of the mean flow and the wake perturbations.

The contribution from a single wake is estimated by an updated version of the Larsen model. As in the original model, the development of the individual wake deficits in the stationary wake model, is governed by the *thin shear layer approximation* of the NS equations, assuming a rotationally symmetric wake deficit, and a homogeneous and incompressible fluid. The extension of the wake in the stationary wake model, is calculated based on boundary conditions related to the value of the rotor plane after pressure recovery, and the mean value at the downstream distance 9.6D, defined by full scale experiments. The imposed boundary conditions also account for the meandering of wakes, which is assumed to have a significant effect on the expansion of the stationary wake field. The first order solutions from equation (2.7) and equation (2.8) in the original Larsen model, is thus updated to

$$R_W^L(x) = \left(\frac{35}{2\pi}\right)^{\frac{1}{5}} (3c_1^2)^{\frac{1}{5}} (C_T A(x+x_0))^{\frac{1}{3}},$$

$$U_{Def}^L(x,r) = -\frac{\overline{U}_\infty}{9} \left(C_T A(x+x_0)^{-2}\right)^{\frac{1}{3}} \left[ r^{\frac{3}{2}} \left(3c_1^2 C_T A(x+x_0)\right)^{-\frac{1}{2}} - \left(\frac{35}{2\pi}\right)^{\frac{3}{10}} \left(3c_1^2\right)^{-\frac{1}{5}} \right]^2,$$

where $\overline{U}_\infty$ is the pseudo-uniform inflow velocity, and $c_1$ and $x_0$ are parameters defined by

$$c_1 = \left(\frac{qD}{2}\right)^{\frac{5}{2}} \left(\frac{105}{2\pi}\right)^{-\frac{1}{2}} (C_T A x_0)^{-\frac{5}{6}},$$

$$x_0 = \frac{9.6D}{\left(\frac{2R_{9.6}}{qD}\right)^3 - 1},$$

where $q$ is a parameter dependent on the thrust coefficient, and $R_{9.6}$ is approximated empirically. Both $q$ and $R_{9.6}$ are resumed in Larsen (2009).

In order to estimate the velocity deficits for individual wakes, a uniform inflow velocity is required. Since the physical inflow field $U$, on a turbine is non-uniform, the pseudo-uniform inflow is in field is Larsen (2009) estimated by two different approaches. The first approach averages the non-uniform inflow wind field over the turbine's rotor swept area by

$$\overline{U}_{\infty} = \frac{1}{A} \int_{A} U dA, \tag{2.9}$$

where, $U$ is described by the logarithmic wind profile from equation (2.1). The second approach is similar to equation (2.9), but also takes the thrust coefficient into account.

By describing the inflow wind field as in equation (2.9), Larsen (2009) derives an expression for calculating the pseudo-uniform inflow field for each downstream turbine affected by upstream wakes.

## 2.4 Optimization methods

Optimization methods are designed to improve an initial solution with respect to a given objective, where the goal is to find an optimal solution to the problem. The objective function specify the intention of the optimization, and is either maximized or minimized during the optimization procedure. For wind farm design optimization problems, the objective is often related to maximizing the annual energy production, minimizing the financial costs, minimizing the foundation costs or minimizing electrical grid costs by changing the location of turbines. Considering the large costs related to installation and operation of offshore wind farms, finding an optimal layout can be crucial for a project's financial profitability. For example, by running an optimization procedure with the AEP as an objective, an increase in production can be attained by relocating turbines away from wakes generated by upstream turbines.

Today, several optimization methods are available, which achieve improved wind farm layouts in different ways. Given that each optimization method only provide good solutions for certain problems, the choice of optimizer is important. In general, the optimization methods can be categorized into three main groups, namely calculus-based methods, heuristic methods and metaheuristic methods. Each type of method contain different strengths and weaknesses, and should thus be chosen based on the characteristics of a specific problem.

### 2.4.1 Calculus-based methods

The calculus-based methods perform exact calculations and are usually applicable to simple problems, where the objective function is differentiable, and the search space is convex and bounded. Some of the common calculus-based procedures are the local search algorithms and the tree-search algorithms. The local search algorithms, including the Newton method and the gradient method, only solve convex problems, as they struggle to overcome local extreme points. According to Herbert-Acero et al. (2014), the tree-search based procedures are considered improved exact techniques, however, their performance is poor when applied to highly constrained models and non-convex search spaces. Thus, in recent research, improvements to the relaxation procedures are further developed, to help overcome this issue.

Another calculus based method applied to wind farm optimization, is the Constrained Optimization BY Linear Approximation (COBYLA), developed by Powell (1994). The COBYLA algorithm is an open source software available at Perez et al. (2012), and is accessible in the TOPFARM library of optimizers. It is a direct search optimization method, applicable for nonlinear derivative-free constrained optimization calculations. During the procedure, each iteration models linear approximations for both the objective and constraint functions, by interpolation at the vertices of a simplex. The variables are restricted to change within a given thrust region for each iteration. The new set of variables are evaluated, and may replace one of the verticies to improve the linear approximations in the proceeding step. When the approximations fail to attain improved variables, the thrust region is decreased to refine the search. The algorithm ends when suffi-

ciently small thrust region values are reached.

### 2.4.2 Heuristic methods

Heuristic methods are developed to provide near-optimal solutions to complex problems. These methods are categorized as relatively fast solvers, but may need to be executed several times in order to guarantee good solutions. There are two different types of heuristic methods, constructive and iterative methods. The constructive methods consider all the defined constraints, and decide the value of each variable based on deterministic or non-deterministic rules. The iterative heuristics improve the complete solution, by evaluating the local search space for each variable involved.

The most basic heuristic algorithm is Random Search (RS). This algorithm randomly samples a number of feasible solutions and determines the best solution from this sample. However, given a specific problem, heuristics which take advantage of the structure of the problem, usually provide better solutions than the RS method. In literature, methods like the Monte Carlo method and the pattern search algorithm, have been successfully adopted in various approaches of the wind farm design optimization problem. In later years, greedy heuristics have also been applied on wind farm optimization problems, and have shown a potential to solve complex wind farm problems (Herbert-Acero et al., 2014).

### 2.4.3 Metaheuristic methods

Metaheuristic methods are designed to find near optimal solutions more efficiently than the heuristic methods, and are defined as high level procedures. According to Herbert-Acero et al. (2014), these optimization procedures are also the most frequently used methods to solve wind farm optimization problems. A typical feature of the metaheuristics is that they are based on behaviour observed in the nature, and hence they perform optimizations by simulating various natural processes.

There are three main groups of metaheuristics, namely construction-based, lo-

cal search-based and population-based methods. The constructive methods build on multiple heuristics to generate a feasible solution. The local search methods assume that feasible solutions of similar quality are related. During the optimization procedure, these methods modify the value of the design variables, resulting in neighbor solutions. In each iteration, the best neighbor solution is selected, and the process is repeated until no better solution is found. Local search algorithms can be powerful solution procedures for wind farm optimization. However, if the search space is too complex, the algorithm may not converge to an optimal solution. An example of a successful local search methaheuristic applied on wind farm optimization problems, is the Simulated Annealing (SA) algorithm. This algorithm mimics the thermal process when heating and cooling cause a solid to melt and then solidify into a new particle arrangement. A special feature with the SA algorithm is that the iterations are allowed to attain less optimal solutions, so that the risk of getting stuck in a local extreme point is minimized (Herbert-Acero et al., 2014).

The most widely used metaheuristic method for wind farm optimization is the population-based Genetic Algorithm (GA). This algorithm exploits the theory that two individuals with the best characteristics in a population can produce a better individual when combined. The performance of the GA is dependent on good choices for the selection and crossover mechanisms (Herbert-Acero et al., 2014).

## 2.5 Wind farm optimization tools

In recent years, various software packages have become frequently used, both with respect to estimating wake influenced wind fields and to optimize wind farm layouts. Since the attained AEP and the wake generation often are considered to be key parameters in the optimization routine, wind resource packages such as WAsP, are often included in commercial software on wind farm optimization. Due to the close relation between wind field software and wind farm optimization software, some relevant products in both areas are described in the following sections.

### 2.5.1 Wind field simulation software

Wind field simulation software often provides a detailed description of the wake behind a single turbine, and turbine clusters. Based on information regarding turbine specifications, atmospheric conditions, and wind data, the programs are able to estimate wake losses and predict the AEP.

#### WAsP

The Wind Atlas analysis and application Program WAsP, developed by the RISØ national laboratory, is designed to describe the wind resource at a given location. The software includes different types of analysis of the wind farm production, the wind farm efficiency, and climate estimations (Herbert-Acero et al., 2014). In addition, a stability model and Katić *et. al*'s wake model, is incorporated in the program (DTU Wind Energy, 2016). Today, WAsP is considered as a standard software for wind resource analysis, and is frequently used for estimating the wind resource at a given site in several optimization software packages, like in WindPro and The WindFarmer v5.2.

#### Fuga

Fuga is a tool developed to estimate the AEP and the wake losses in offshore wind farms, and is available as an additional package to the software WAsP. Due to the assumption of a horizontally homogeneous atmospheric boundary layer, Fuga is best applied to wind farms located offshore.

A central component in Fuga is the flow model, which is categorized as a linearized CFD model. The model consists of simplified equations derived from original CFD models, and calculates the linear responses to the turbine thrust forces, with a simple turbulence closure. The solutions obtained by Fuga do not describe the near wake field accurately, but provide a sufficiently accurate description for the far wake region, with respect to predicting the AEP. In addition, the program is estimated to be $O(10^5)$ times faster than original CFD models (DTU Wind Energy, 2015). One of the reasons why the program is so fast is the inclusion of

general and turbine specific look-up tables, used to construct velocity fields behind the turbines.

For multiple turbines, the combined wake effect is estimated by the sum of all wake perturbations. The description of Fuga by Ott et al. (2011), does not take the effect of meandering into consideration. Therefore, wider wind direction bins are proposed to reduce meandering errors.

### 2.5.2 Wind farm optimization software

A common feature of the various wind farm optimization tools is that they often offer a detailed optimization analysis, including several variables such as noise impact, shadow flicker, visual impact, electrical grid costs, foundation costs or wake loads, in addition to the AEP calculation (Herbert-Acero et al., 2014). By including multiple parameters, a more realistic evaluation of the wind farm optimization is maintained and better results are generated.

One of the tools available for wind farm optimization is TOPFARM, which is developed to optimize a layout from a cost perspective. The program is able to solve problems based on a multi-fidelity approach, where optimization routines of increasing complexity are run in several steps, to attain an optimal solution (Réthoré et al., 2014). Other software packages which are frequently used in the wind community include WindPRO and The WindFarmer v5.2, both performing optimizations with the AEP as an objective (Herbert-Acero et al., 2014).

#### WindPRO

The WindPRO optimization software is developed by EMD International A/S, where WAsP is incorporated in the program to perform an evaluation of the wind resource. In the program, several different modules are included like the simulation and quantification of the energy production, environmental impacts and electrical layout design. The optimization procedure is based on greedy heuristics, and takes in the AEP as a performance metric. Several optimization processes are available in the program, all based on a pre-calculated wind resource map from WAsP. One

approach is based on adding turbines in the wind farm to fixed positions, until an upper limit is met. Alternatively, a modification of the wind farm layout can be performed, by changing the separation distance between turbines.

#### The WindFarmer v5.2

The WindFarmer v5.2 is a tool developed by DNV GL, and is similar to WindPRO, as it includes WAsP for wind resource quantification. In this model, the wake loss is estimated by using a CFD model, with an eddy viscosity as turbulence closure. The optimization procedure is based on greedy heuristics, either by optimizing the AEP, or the financial balance of the project.

## 2.6 TOPFARM

TOPFARM is a tool for wind farm layout optimization, developed in the EU project lead by Risø National Laboratory, which takes in a project's total economical benefits as an objective. Thus, the balance between the income from power production versus various wind farm expenses like installation costs, operation and maintenance costs and fatigue degradation is evaluated. The TOPFARM project is organized into eight work packages which focus on various technical topics, such as the basic modules of the TOPFARM optimization platform, verification of submodels, and demonstrations of the optimization method for onshore and offshore sites. A further description of each work package is available in the report by Larsen et al. (2011).

The four basic modules in the TOPFARM optimization platform are

1. Wind farm flow field modelling
2. Aero-elastic modelling of the wind turbines
3. Cost modelling
4. Optimization.

The first module on flow field modelling provides a library of different wake models, including the simple stationary semi analytical wake model (see Section 2.3.2) and a dynamic wake meandering model, amongst others. The available models describe the flow field in varying detail, where the choice of model is dependent on the problem at hand. Given that the first approach uses a detailed wind field wake model, like the dynamic wake meandering model, the second module can provide aero-elastic load and production calculations. The third module evaluates the income and expenses of a project, using simple cost models such as maximizing the annual energy production versus minimizing foundation costs, electrical grid costs or fatigue degradation costs. In order to generate an optimal solution, the first three modules are incorporated into the last module. This module contains a library of several optimization algorithms, which are selected depending on the characteristics of the problem (Larsen and Réthoré, 2013).

For the optimization in TOPFARM, a multi-fidelity approach is suggested, including three levels of fidelity. In this way, the majority of the problem can be solved by applying a fast and approximate model, while a detailed and more accurate model is applied to refine the search in specific interesting regions. The first fidelity level is constructed to perform an energy production optimization, where the AEP is calculated using a simple wake model, such as the simple stationary semi analytical wake model. In Réthoré et al. (2014), cost models on the foundation and electrical grid is also included in the first fidelity level. The second fidelity level includes pre calculated look-up tables for a number of load cases, and enables the inclusion of a wake induced fatigue-degradation cost function in the optimization. The complex third fidelity level include full aero-elastic load calculations combined with wake meandering, directly in the optimization procedure.

The possibility of including various components in the optimization like AEP, wake loads, foundation costs and cable costs enables the generation of realistic layout solutions. TOPFARM also differs from most optimization programs as it includes costs related to wake loads. While most optimization software evaluates the wake in terms of production loss, the load on individual turbines due to wake is rarely considered.

# Chapter 3

# Method

## 3.1 Constructing a TOPFARM model

Due to time limitations and the size of the case study, expenses related to wind farm construction and operation are defined out of scope. In this thesis, TOPFARM is thus used to optimize the layout with only the AEP as an objective, for the planned offshore wind farm Creyke Beck B. For this purpose, a general model is created in an Ipython notebook, and used as a basic structure when constructing various experiments. The model is based on a subset of the available class functions in the TOPFARM library, and performs layout optimizations to improve the AEP. The model also requires certain data input, such as wind conditions, turbine specifications, initial layouts and wind farm border points, in order to run. Figure 3.1 gives an overview of the structure of the model.

The imports in the model, shown in Figure 3.1, are extracted both from the existing TOPFARM library, and from implementations added to the code, documented in Section 3.3. Further on, the model takes in and organizes the data from Section 3.2. All initial information such as wind turbine layout and the wind resource are plotted inside the notebook. The proceeding step calculates the initial AEP, using the stationary semi analytical wake model, the wind resource data, and the turbine specifications. The accuracy of the AEP calculation is decided by the user, by determining the resolution of the wind speeds and wind directions used to estimate the production. The chosen resolution denotes the discretization of the

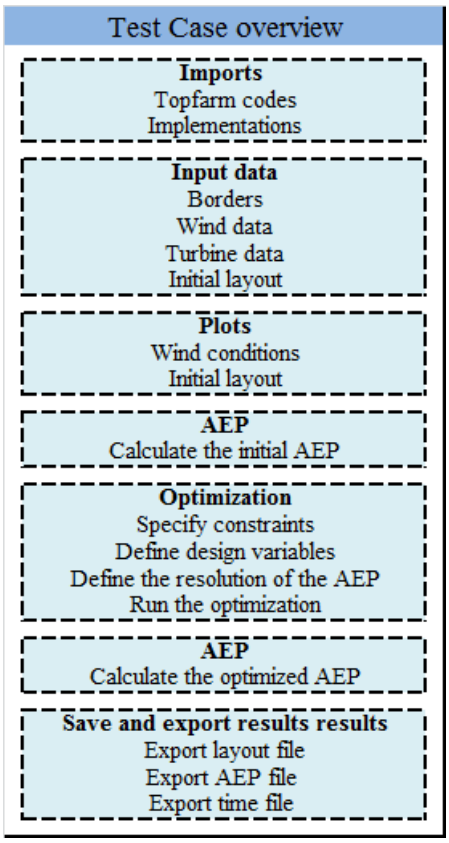


Figure 3.1: The general structure of the model.

wind speeds and wind directions within the given ranges of 4 m/s and 25 m/s, and 0 degrees and 360 degrees, respectively. Since the first and last value in the wind direction range denote the same direction, the last wind direction value attained by the dicretization, is disregarded. For the initial layout, a resolution of 21 wind speeds and 181 wind directions are chosen, resulting in an AEP calculation with a relatively high accuracy.

Prior to the optimization routine, various constraints must be specified. In addition, choices such as the number of variables, the quality of the AEP calculation, and the optimizer are decided here. Since AEP calculations of high accuracy are computationally demanding, the resolution of the wind speeds and wind directions are significantly reduced in the optimization routine. The optimizer chosen in the thesis, is a constrained optimization by linear approximations called COBYLA, which performs linear approximations of both the objective and the constraint functions. After the optimization, the AEP is calculated for the optimal wind farm layout, with the same resolution as in the initial layout. The production and

layout results are then saved and exported as separate files.

## 3.2 Data

TOPFARM requires input-data for wind conditions, turbine specifications, initial layouts, and the wind farm border points in order to perform an optimization for Creyke Beck B. To provide an overview of the content of the various data, this subsection present a description of the various input parameters.

### 3.2.1 Turbine spesifications

Data from the Technical University of Denmark's (DTU) 10MW Reference wind turbine are used to provide the required turbine specifications in the thesis. This is a virtual turbine, designed by the Wind Energy Department at DTU, and Vestas (Bak et al., 2013). Due to the turbine's highly detailed description and publicly available data, it is assumed to be a suitable wind turbine choice.

Inside the TOPFARM functions, turbine specifications are included by importing a '.wtg' file with the necessary input. This type of file is primarily known from WAsP, as a data file containing power and thrust curves for a specific wind turbine. By using the available data, a '.wtg' file for DTU's 10MW turbine is constructed. In this file, turbine information from Table 3.1 taken from Table 2.1 in Bak et al. (2013, p.13), and tables on the turbine's thrust and power performance taken from Table 3.5 in Bak et al. (2013, p.34), are included. In the technical report, only the turbine's mechanical power performance is listed. To account for the energy loss related to conversion from mechanical power to electrical power, the performance included in the '.wtg' file is consequently lowered by 0.6 MW. It is noted that this adjustment may under-predict the generated power from lower wind speeds. Figure 3.2 gives a graphical representation of the wind turbine's performance, which is included in TOPFARM.

| Parameters | DTU's reference turbine |
|---|---|
| Rated power | 10 MW |
| Cut in wind speed | 4.0 m/s |
| Rated wind speed | 11.4 m/s |
| Cut out wind speed | 25.0 m/s |
| Number of blades | 3 |
| Rotor diameter | 178.3 m |
| Hub height | 119.0 m |

Table 3.1: Key parameters for DTU's 10 MW reference wind turbine.

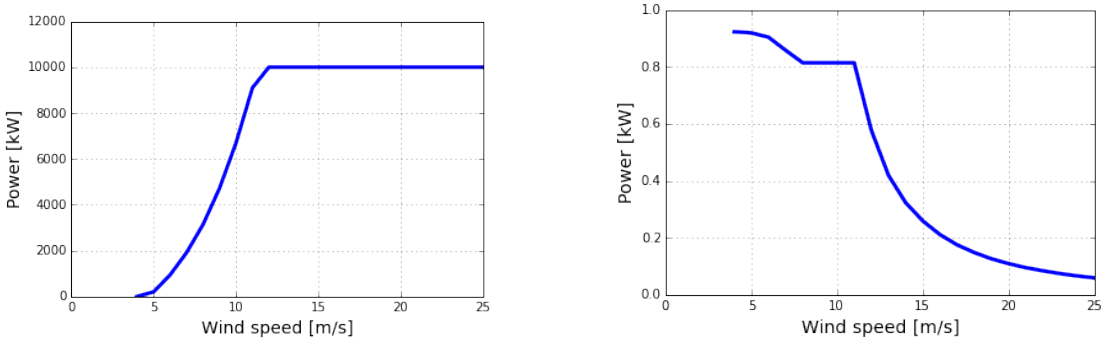


(a) Power curve

(b) Thrust coefficient curve

Figure 3.2: Performance curves for DTU's 10MW reference turbine.

### 3.2.2 Wind data

Nora10 is an archive which provides a hind-cast of wind and wave data in the North Sea, the Norwegian Sea and the Barrents Sea (Reistad et al., 2007). In order to obtain and analyse the wind conditions at Dogger Bank, data for a coordinate point in Creyke Beck B (5493N,0165E) has been extracted from this archive, with the assistance from the Norwegian Meteorological Institute. The data series contain one hourly averaged measurements for wind and wave conditions, in a time span ranging between the years 1957 and 2015. In Table 3.2, a subset of the available data is listed, where all Nora10 wind data are included.

The wind conditions at a given location vary with altitude. In order to obtain realistic power estimations, the chosen wind data must therefore represent the

| Name | Denom. | Description |
|---|---|---|
| Y | | Year |
| M | | Month |
| D | | Day |
| H | | Hour |
| T2m | (°C) | Air temperature 2 m above sea level |
| RH2m | (%) | Relative humidity 2m above sea level |
| W10 | (m/s) | Wind speed 10 m above sea level |
| W50 | (m/s) | Wind speed 50 m above sea level |
| W80 | (m/s) | Wind speed 80 m above sea level |
| W100 | (m/s) | Wind speed 100 m above sea level |
| W150 | (m/s) | Wind speed 150 m above sea level |
| D10 | (°) | Wind direction 10 m above sea level |
| D100 | (°) | Wind direction 100 m above sea level |
| D150 | (°) | Wind direction 150 m above sea level |

Table 3.2: A subset of the available data from Nora10.

wind conditions at the altitude where the power is extracted. Given DTU's 10MW reference wind turbine with a measured hub height of 119 m, corresponding wind conditions representing this altitude are needed. Nora10 does not contain wind data at this particular altitude, and values of the wind speeds and wind directions at 119 m are therefore estimated.

### Estimating wind data

For long term statistical estimations, the wind shear in equation (2.1) is expected to depend mostly on the surface roughness (Hau, 2006). A simplified estimation of the wind shear which is frequently used in the wind industry, expressed as

$$U(z) = u_1 \left( \frac{z}{z_1} \right)^{\beta}, \tag{3.1}$$

is therefore used for estimating the wind data at the desired reference height. Here, $u_1$ represents the wind speed at reference height $z_1$, $U(z)$ represents the estimated wind speed at altitude $z$, and $\beta$ is an empirical wind shear parameter. The value

of $\beta$ is dependent on the surface roughness at a location, with an approximated value of $\beta = 0.1$ for an open sea (Hau, 2006).

The wind directions at altitude $z$ are estimated by evaluating the change between the wind directions at two known altitudes, $z_1$ and $z_2$, where $z_2 > z > z_1$. In Nora10, the directional values range between 0 and 360 degrees, where 0 and 360 both denote winds from the north. Due to this notation, the directional change in degrees must be carefully evaluated, where the smallest change in a polar coordinate system is chosen. Thus, given two unit vectors $d_1$ and $d_2$ with the corresponding directions $\alpha_1$ and $\alpha_2$ at reference altitudes $z_1$ and $z_2$, the angular difference between them is given by $\theta = |\alpha_2 - \alpha_1|$ and $\phi = 360 - \theta$, as shown in Figure 3.3

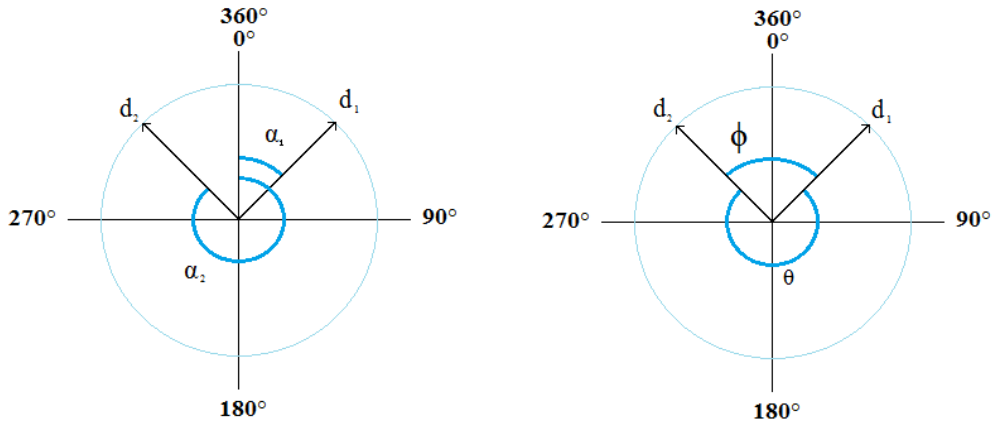


Figure 3.3: Illustration of two wind directions at altitudes $z_1$ and $z_2$, and the angular difference between them.

To determine the change in wind direction between the altitudes $z_1$ and $z$, the smallest angular distance is multiplied with the relative change in height between $z_1$, $z_2$, and $z$ as follows

$$\Delta\alpha(z) = min(\theta, \phi)\frac{z - z_1}{z_2 - z_1}. \tag{3.2}$$

By adding the change in direction $\Delta\alpha(z)$, with $\alpha_1$ at reference level $z_1$, values for the wind direction $\alpha(z)$ at hub height $z$ is determined by

$$\alpha(z) = \begin{cases} \alpha_1 + \triangle\alpha, & \text{if } \alpha_2 \geq \alpha_1 \text{ and } \phi \geq \theta \\ \alpha_1 - \triangle\alpha, & \text{if } \alpha_2 \geq \alpha_1 \text{ and } \phi < \theta \\ \alpha_1 - \triangle\alpha, & \text{if } \alpha_2 < \alpha_1 \text{ and } \phi \geq \theta \\ \alpha_1 + \triangle\alpha, & \text{if } \alpha_2 < \alpha_1 \text{ and } \phi < \theta. \end{cases} \tag{3.3}$$

In order to generate wind data at 119 m, Nora10 data for 100 m elevation and 150 m elevation are used. An array of suitable wind speed values is estimated, by applying equation (3.1) for each entry in the array 'W100' from Table 3.2. Corresponding directions are estimated, by calculating the directional change between each corresponding entry in 'D100' and 'D150' from Table 3.2, using the equations (3.2) and (3.3). The result is a data set of wind speeds and wind directions, which can be used to further analyse the wind resource at Creyke Beck B.

**Preparing the input data**

In TOPFARM, the wind data are represented by a Weibull matrix, containing 12 wind directions. For each direction, the matrix includes the occurring frequency of each direction, and two Weibull function parameters, namely the scale parameter $\eta$, and the shape parameter $\kappa$. Based on these parameters, a Weibull distribution representing the probabilities of different wind speeds in a given direction can be generated. The Weibull distribution is expected to provide a good fit for the wind speed observations in each direction, and is a computationally inexpensive way of storing the wind information (Ehrlich, 2013).

In the process of transforming the wind data at 119 m altitude into a Weibull matrix, the data are sorted into bins for 12 wind directions and 40 wind speeds. For each directional bin, a Weibull fit is performed to generate shape and scale parameters. The results are saved as a simple Weibull matrix as shown in Table 3.3.

### 3.2.3 Border coordinates

The coordinate points for the Creyke Beck B border are extracted from Table 2.5 in the technical report by Forewind (2013a, p.15). In this report, the borders are

| Direction | Frequency | Scale $\eta$ | Shape $\kappa$ |
|---|---|---|---|
| 0 | 0.069 | 9.97 | 2.17 |
| 30 | 0.047 | 8.74 | 2.14 |
| 60 | 0.048 | 9.56 | 2.14 |
| 90 | 0.054 | 10.52 | 2.19 |
| 120 | 0.059 | 10.68 | 2.20 |
| 150 | 0.067 | 10.73 | 2.26 |
| 180 | 0.094 | 11.78 | 2.30 |
| 210 | 0.127 | 12.76 | 2.38 |
| 240 | 0.133 | 12.83 | 2.38 |
| 270 | 0.117 | 12.29 | 2.21 |
| 300 | 0.092 | 11.21 | 2.13 |
| 330 | 0.093 | 11.25 | 2.22 |

Table 3.3: A Weibull matrix for wind data at 119 m elevation in Creyke Beck B.

given by eastling and northling points in the Universal Transverse Mercator (UTM) coordinate system. The border points used as input in TOPFARM shown in Table 3.4, are translated to fit a coordinate system where $(x, y)\ \epsilon\ [0, 30000]$, with meters as unit. Since the UTM coordinates are measured in meters, this transformation is simply performed by subtracting each point with a constant value.

| Point | x | y |
|---|---|---|
| CBB-1 | 4999 | 27085 |
| CBB-2 | 8351 | 27417 |
| CBB-3 | 15756 | 29740 |
| CBB-4 | 27362 | 29740 |
| CBB-5 | 27362 | 2703 |
| CBB-6 | 2487 | 4481 |
| CBB-7 | 3675 | 15258 |
| CBB-8 | 3658 | 15702 |

Table 3.4: Border points for Creyke Beck B.

### 3.2.4 Initial layouts

The initial layouts used in the various experiments, are constructed in a separate Ipython notebook. Here they are saved as '.out' files, so that they can be used as initial layout input in the model. In this study, different layouts are generated and used as initial layouts for various experiments. Two of these are constructed based on layout suggestions by Forewind (2013a) for Creyke Beck B. The suggested layouts in the report includes 300 4 MW wind turbines and 7 offshore platforms (see Section 2.2.2). In this thesis however, the layouts consist of 120 10 MW turbines, and do not include offshore platforms. In addition, the wind farm's convex hull has been added as a feasible area, to create a convex wind farm (see Section 3.3.1). As a result, the initial layouts generated in the thesis are not identical to Forewind's proposed layouts.

#### Layout 1

One of the suggested layouts for Creyke Beck B by Forewind (2013a, p.173), consists of turbines on the wind farm perimeter together with a uniform grid inside the wind farm. Layout 1 in Figure 3.4 is a recreation of the suggested layout, for a set of 120 10MW wind turbines. It is constructed to contain the same ratio of wind turbines on the perimeter and inside the borders as the layout from the report.

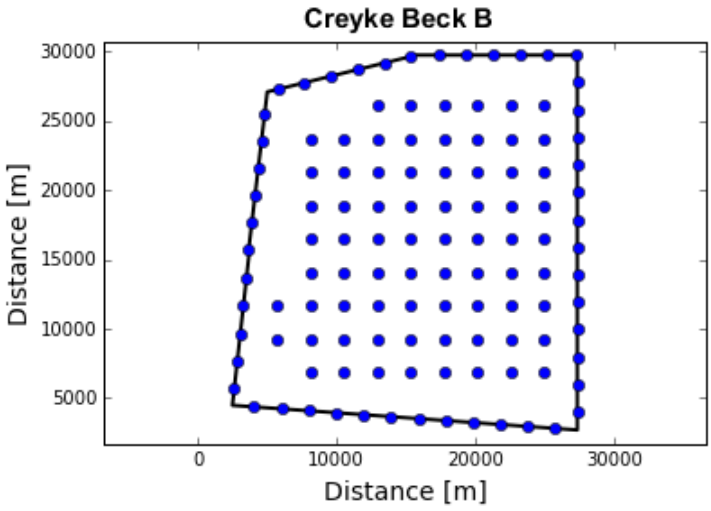


Figure 3.4: Layout 1.

### Layout 2

Layout 2 is a recreation of a layout suggested by Forewind (2013a, p.174), and have the same ratio of turbines inside and on the border. The placement of the turbines in Layout 2 is similar to Layout 1, but with fewer columns, and with a closer turbine spacing as shown in Figure 3.5.

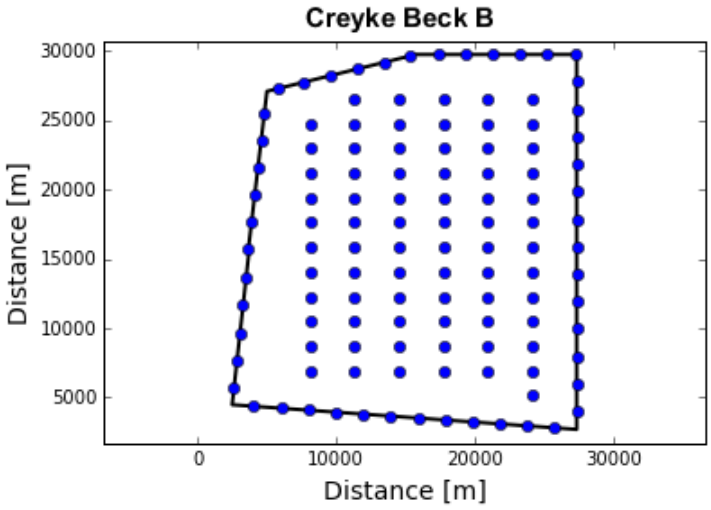


Figure 3.5: Layout 2.

### Layout 3

In Layout 3 the turbines are spread out over the available area in a rectangular grid, as shown in Figure 3.6. Despite the simple structure, rectangular grid layouts are seen in several commissioned wind farms, like Hornes Rev 1 and Amrumbank West (4C Offshore, 2013), and it is therefore interesting to evaluate this layout structure further.

### Layouts distributed over smaller areas

Apart from the turbine spacing and number of columns and rows chosen, the layouts distributed over smaller fractions of the Creyke Beck B area are identical to Layout 3. In total, six initial layouts utilizing different fractions of the available area are generated, utilizing 80%, 70%, 60%, 50%, 40% and 30% of the original Creyke Beck B area, respectively. The reduced areas are restricted to fit into the original Creyke Beck B borders, where the borders are chosen based on

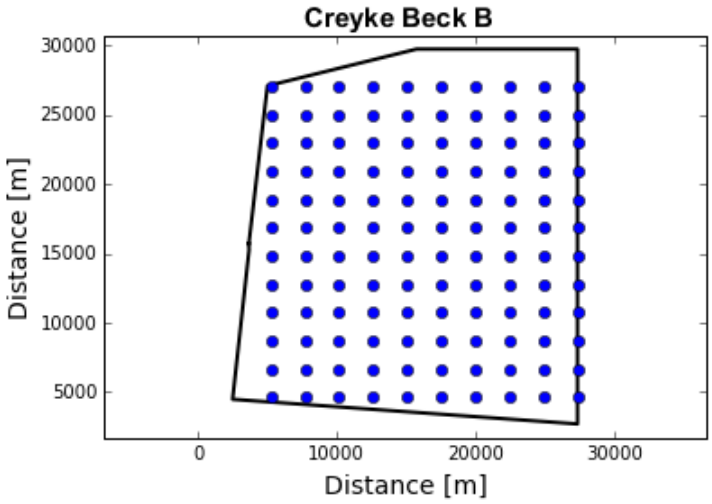


Figure 3.6: Layout 3.

empirical evaluations on attaining the highest AEP. Figure 3.7 gives an overview of each initial layout generated, compared to the original borders. Each initial layout is named after the percentage of the original Creyke Beck B area utilized, thus attaining the names CBB80, CBB70, CBB60, CBB50, CBB40 and CBB30, respectively.

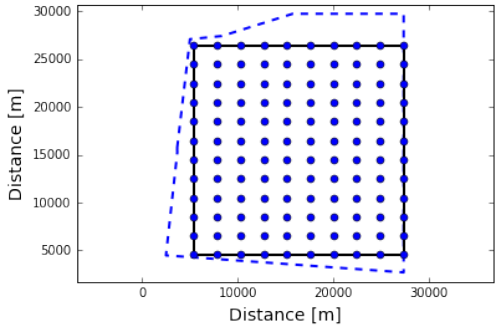


(a) 80% of the available area.

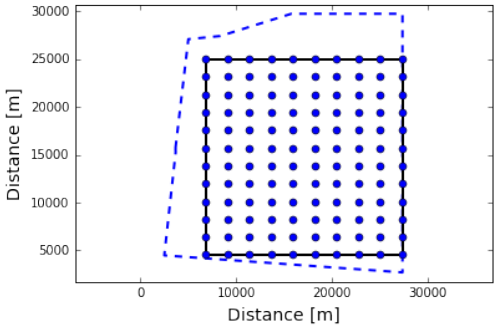


(b) 70% of the available area.

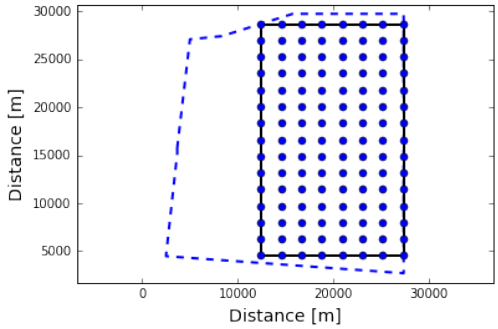


(c) 60% of the available area.

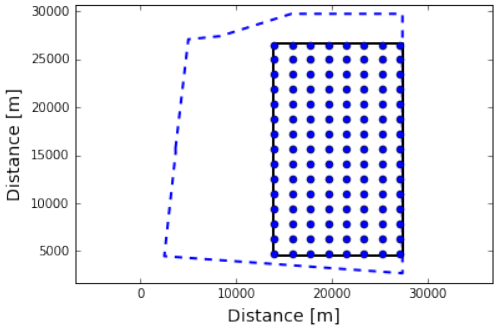


(d) 50% of the available area.

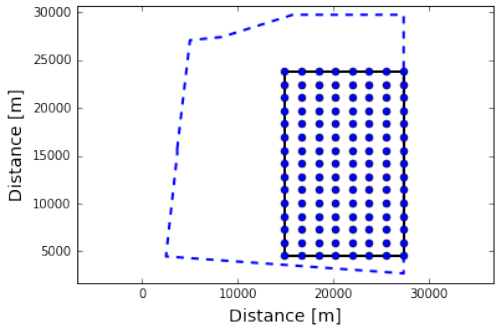


(e) 40% of the available area.

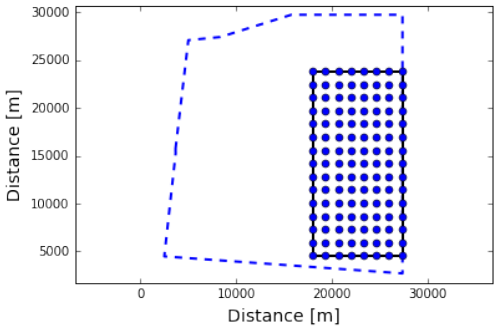


(f) 30% of the available area.

Figure 3.7: Layouts distributed over smaller fractions of Creyke Beck B, with the dashed lines illustrating the original borders.

## 3.3 Topfarm implementations

Due to the fact that TOPFARM is constructed for significantly smaller test cases than the planned wind farm Creyke Beck B, some difficulties with the optimization were expected. Early in the implementation process it became clear that optimizing the location of all 120 turbines, was too computationally demanding.

Another issue appeared for smaller test cases which were able to run, but where some constraints were ignored by the program. In addition, the energy production after the optimization often ended up being lower than the initial production. Based on these observations, three main challenges were identified for enabling the optimization routine to run for Creyke Beck B:

1. Get TOPFARM to respect the constraints
2. Get TOPFARM to handle the required amount of turbines.
3. Get TOPFARM to perform AEP calculations of improved quality.

In this section, various implementations are presented, where each implementation is constructed to accomplish one of the challenges stated above. TOPFARM's ability to run is highly influenced by the number of variables included in the optimization, and the number of included constraints. Therefore, limiting these numbers has been a priority when defining the implementations, where a reduction in the number of variables included in the optimization, is addressed in Section 3.3.3. The total number of constraints generated in one optimization run, when including the various implementations is expressed by

$$\text{Const}_l = \text{Border}_l + \text{Dist}_l - \text{Fixed}_l, \quad l = 1, 2. \tag{3.4}$$

Here, $\text{Const}_l$ is the total number of constraints, dependent on the border constraints $\text{Border}_l$ (see Section 3.3.1), the turbine distance constraints $\text{Dist}_l$ (see Section 3.3.2) and the reduction from the fixed turbine constraints $\text{Fixed}_l$ (see Sections 3.3.3 and 3.3.4). This general expression is valid for two different cases, where the value of $l$ denotes each case. Case 1 is based on an optimization where the turbines can move freely, with wind farm borders and turbine spacing as the only restrictions. Case 2 includes some restrictions in the optimization for the turbine movement, where the turbines can move within either its row or column. In addition, each row or column must preserve the order of the wind turbine placement throughout the optimization. In this thesis, only the number of constraints generated by the column optimization are presented.

### 3.3.1 Border constraints

In TOPFARM, a wind farm polygon is constructed from a set of border points which are generated manually by the user. When creating a new array of points, the user may start anywhere. However, it is expected that the subsequent points are arranged in order, moving in a clockwise direction around the border. In addition, the starting border point must also be the last point in the array.

A wind farm layout is feasible only if all the turbines are positioned inside the defined wind farm area. For a convex $s$-sided polygon, such an area can be described by the following set of linear constraints

$$-a_k x + b_k y \leq C_k, \quad k = 1, \ldots, s, \tag{3.5}$$

where $a_k$, $b_k$, and $C_k$ are constants, $s$ is the number of polygon edges, and $x$ and $y$ are arbitrarily chosen coordinate points. In an optimization run for Case 1, the total number of border constraints needed are

$$\text{Border}_1 = s * T, \tag{3.6}$$

where $T$ is the total number of wind turbines. Assuming a convex wind farm, Case 2 only needs to consider the first and the last turbine in each column, thus the number of constraints is

$$\text{Border}_2 = s * 2c, \tag{3.7}$$

where $c$ denotes the number of columns in the layout.

To maintain consistency, the number of border constraints generated by Case 1, will be used further on in this section. When adding a string of border constraints in TOPFARM based on the equations (3.5) and (3.6), the inequalities added in the optimization are expressed by

$$\begin{aligned} -a_k x_i + b_k y_i \leq C_k, \quad & k = 1, \ldots, s \\ & i = 1, \ldots, T, \end{aligned} \tag{3.8}$$

where $(x_i, y_i)$ is the coordinate pair for the location of turbine $i$.

### Handling non-convex wind farms

Equation (3.5) is only applicable to convex wind farm polygons. Otherwise, the inequalities will exclude some areas within the wind farm which are in fact feasible. Figure 3.8 illustrates this, on the non-convex wind farm Creyke Beck B. To avoid the exclusion of certain areas, vertices generating non-convex areas must therefore be identified.

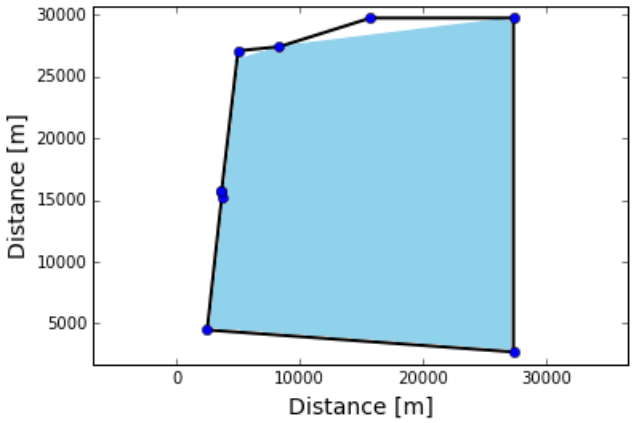


Figure 3.8: Feasible area (in blue) for Creyke Beck B when using linear border constraints.

If each vertex has an angle less than 180 degrees inside the wind farm area, then the shape of the wind farm is convex. When evaluating an angle between two vectors in Python, the smallest angle is automatically chosen. Therefore it is not possible to know if this angle represents the inside or the outside of the feasible area. To make sure that the inside of the feasible area is calculated, an alternative method is introduced.

A set of $s$ border line vectors are created, based on the border coordinates $(x_k, y_k)$. Since the vectors are directed clockwise around the border, an arbitrary vector $v_k$ given by

$$v_k = (x_{k+1} - x_k, y_{k+1} - y_k)$$

will for a convex vertex have the next vector $v_{k+1}$ located to the right. In addition, the corresponding normal vector $w_k$ given by

$$w_k = (y_{k+1} - y_k, x_k - x_{k+1})$$

is located to the right of the border line vector $v_k$ as illustrated in Figure 3.9.

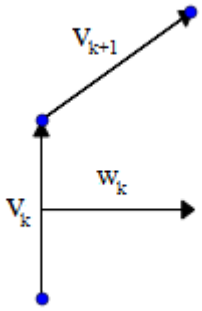


Figure 3.9: Illustration of the relation between $v_k$, $v_{k+1}$ and $w_k$ at a convex vertex.

Therefore, the angle for each vertex is determined by calculating the angle between $v_{k+1}$ and $w_k$. If both vectors are located to the right of $v_k$ the angle between them is less than 90 degrees, and the wind farm is convex at vertex $k$. After evaluating each vertex, vertices generating non-convex areas are eliminated as border points. As a result, the wind farm borders are changed, and the convex hull from the original wind farm becomes the new feasible area, as shown in Figure 3.10 for Creyke Beck B.

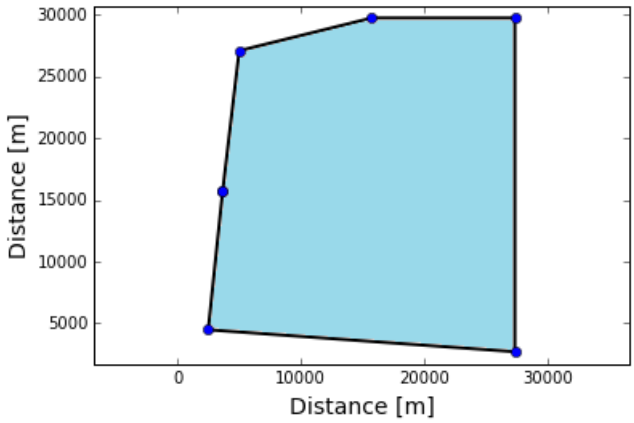


Figure 3.10: The feasible area (in blue) inside a convex Creyke Beck B area.

### Implementing border constraints in TOPFARM

Prior to the constraint implementation, the constants $a_k$, $b_k$ and $C_k$ are calculated for each border line. These values are obtained by solving equation (3.5) as equality constraints, with respect to y coordinates, which can be written as follows if $b_k \neq 0$

$$y = \frac{a_k}{b_k}x + \frac{C_k}{b_k}, \quad k = 1, \ldots, s. \tag{3.9}$$

Since $a_k$, $b_k$ and $C_k$ are all constant values, only the ratios between them are needed, and $b_k$ is set to 1. The remaining constants, $a_k$ and $C_k$, are determined by exploiting the given boundary points. For $b_k = 1$, $a_k$ is equal to the growth-rate of border line $k$, which gives

$$a_k = \frac{y_{k+1} - y_k}{x_{k+1} - x_k}, \quad k = 1, \ldots, s,$$

where the coordinate points $(x_{k+1}, y_{k+1})$ and $(x_k, y_k)$ are the boundary points corresponding to the $k$th border line, and $(x_{s+1}, y_{s+1}) = (x_1, y_1)$. $C_k$ is determined by solving equation (3.9) with respect to $C_k$, by including the corresponding boundary coordinate point $(x_k, y_k)$.

Equation (3.9) applies to all lines, except for vertical lines where $b_k = 0$. From equation (3.5) this exception can be expressed by

$$-a_k x = C_k \quad k = 1, \ldots, s. \tag{3.10}$$

The ratio between $a_k$ and $C_k$ is then found by choosing $a_k = -1$, which leads to $C_k = x$. As the line is vertical, the value of $x$ is constant for all border line points.

Before the calculated values for $a_k$, $b_k$ and $C_k$ are implemented in equation (3.8), the sense of the inequality is to be determined. Depending on the value of $b_k$, this is done by solving equation (3.9) or equation (3.10) for a border point which is not located on the current border line. The inequality that generates a true expression is then chosen. If the calculated value is greater than $C_k$, all three constants are multiplied with $-1$ before being implemented in equation (3.8). This is done so that all the constraints are expressed with the same inequality sign.

### 3.3.2 Turbine distance constraints

The wake behind a wind turbine is greater for larger rotors, and therefore a larger spacing is required. According to Forewind (2013a) the minimum wind turbine spacing required for 10 MW turbines is 6D. Depending on the allowed relocation of turbines, different sets of wind turbine distance parameters are required.

For wind farm optimization where the relocation of turbines is restricted only by the border constraints as in Case 1, each turbine must according to the spacing

rule be located a minimum of 6D away from all other turbines inside the defined area. This is achieved by the following set of constraints

$$\sqrt{(x_i - x_j)^2 + (y_i - y_j)^2} \geq 6D \quad i, j = 1, \ldots, T \\ j > i,$$

for each distinct wind turbine pair with the coordinates $(x_i, y_i)$ and $(x_j, y_j)$. The total number of wind turbine distance constraints $\text{Dist}_1$ for Case 1 are thus

$$\text{Dist}_1 = \sum_{n=1}^{T} (T - n) = \frac{T(T-1)}{2}. \tag{3.11}$$

In Case 2, the number of distance constraints is reduced compared to Case 1, since each turbine only needs to respect the distance to the neighbor turbines in the same column. Therefore, an acceptable turbine distance within each column is maintained by the following set of equations when $x_i - x_{i-1} = 0$

$$y_i \geq y_{i-1} + 6D, \quad i = 2, \ldots, T$$

If $x_i - x_{i-1} \neq 0$, no constraint between the turbine pair is needed, as they are located in different columns. The resulting number of constraints generated for Case 2, is thus

$$\text{Dist}_2 = T - c. \tag{3.12}$$

### 3.3.3 Fixed turbine positions

A method enabling TOPFARM to handle larger wind farm cases, is to run the optimization with a set of turbines at fixed positions. In this way, the number of variables in the optimization can be significantly reduced, resulting in a less demanding optimization run. Given that only a subset of the wind turbines are relocated when including turbines at fixed positions, several optimization steps are required to relocate all the turbines. For each step, a new set of wind turbine variables are chosen, where the number of optimization steps is dependent on the number of defined variables.

TOPFARM's original design includes all the wind turbines as variables. Introducing a set of fixed turbines therefore requires changes to a class named 'DistributeXY()' in the TOPFARM library. The purpose of this class is to save and

update the current wind turbine layout throughout the optimization. Turbines at fixed positions are included in the class by defining two different layouts, one including only the turbines introduced as variables, and the other including all the turbines in the layout. In addition, a list of numbers corresponding to each variable's placement in the original layout is included, so that the positions of the correct turbines are updated during each iteration.

By introducing turbines at fixed positions in the optimization, the number of constraints in each optimization step is reduced, as generating border constraints for fixed turbines is excessive. In addition, constraints related to the turbine distance between two turbines at fixed positions can be neglected. For Case 1, the achieved reduction in constraints by including fixed turbines is thus

$$\text{Fixed}_1 = T_f * s + \sum_{n=1}^{T_f}(T_f - n) = T_f * s + \frac{T_f(T_f - 1)}{2}, \tag{3.13}$$

where $T_f$ denotes the number of fixed wind turbines. The first part of the equation represents the reduction in border constraints, and the second part represents the reduction in turbine distance constraints. By combining the equations (3.6), (3.11) and (3.13), the total number of constraints generated for Case 1 from equation (3.4) are

$$\text{Const}_1 = s(T - T_f) + \frac{1}{2}(T(T-1) - T_f(T_f - 1)).$$

Given that the turbines in Case 2 are restricted to relocate within the columns, constraints for each variable are added in the optimization to ensure that the $x$ coordinate for each turbine is fixed. Thus for each turbine defined as a variable, the following set of constraints are included

$$x_j = D_j, \quad j = 1, \ldots, (T - T_f), \tag{3.14}$$

with $D_j$ denoting the initial $x_j$ coordinate for the $j$th variable. Since the model only considers inequality constraints, each variable creates two constraints. Apart from this, a reduction in constraints with respect to both turbine distance constraints and border constraints are generated by fixing the turbines. Given that all turbines within a column are either set to be fixed or to be a variable, all constraints related to fixed turbine columns can be disregarded. By combining the constraints added by fixing turbines to specific columns from equation (3.14)

with the attained reduction in constraints, the total reduction in constraints by including fixed turbines for Case 2 is given by

$$\text{Fixed}_2 = 2c_f * s + (T_f - c_f) - 2 * (T - T_f), \tag{3.15}$$

where $c_f$ denotes the number of fixed columns in the optimization step. The first and second part of the equation represent the reduction in border and turbine distance constraints, respectively, while the third part of the equation is related to the added constraints from equation (3.14). By combining the equations (3.7), (3.12) and (3.15), the total number of constraints generated for Case 2 from equation (3.4) are

$$\text{Const}_2 = (c - c_f)(2s - 1) + 3(T - T_f).$$

### 3.3.4 Wind farm subareas

Despite the inclusion of fixed turbines in the code, running TOPFARM for Case 1 is challenging due to the large number of constraints generated. To reduce the number of constraints even further, the original wind farm is therefore divided into a set of subareas for this case. Based on the structure of the initial layouts for Creyke Beck B, two different methods for dividing the area are constructed. The first method is applicable for experiments where layouts distributed as rectangular grids are used as initial layout, like Layout 3. The second method is used for experiments with Layout 1 and Layout 2 as initial layouts.

In both methods, new border points are specified to divide the wind farm into smaller areas. Once the additional points are determined, a unique set of border points are generated for each subarea. As for the original border, the subarea borders are arranged in a clockwise manner with the first point and the last point in the array being equal. After generating these, the order of the turbines in the initial layout is sorted by subarea.

The subareas used for Layout 3 and the layouts constructed for smaller fractions of the Creyke Beck B area, are shown in Figure 3.11. Here, $m$ subareas are constructed, where the open space between each area is given by the minimum

accepted turbine distance. In this way, the wind turbines inside one subarea are always located a distance > 6D away from the turbines inside the neighbouring subareas.

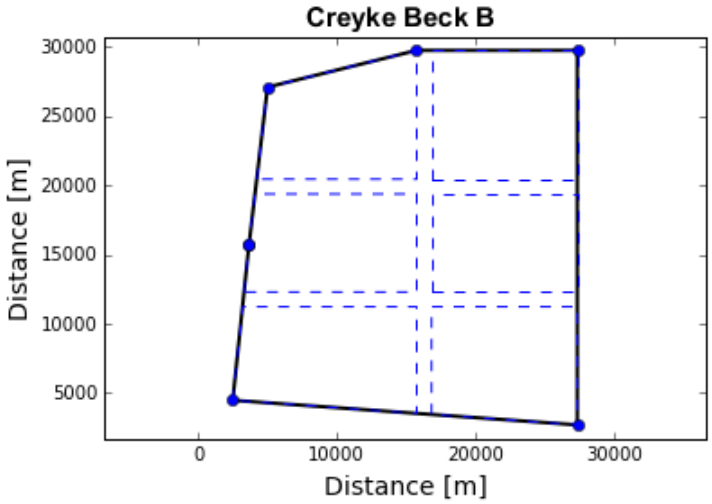


Figure 3.11: Subareas for rectangular grid layouts.

For Layout 1 and Layout 2, the generated subareas in Figure 3.12, have no empty space between them. Therefore, the distance between the turbines and their respective subarea borders must be evaluated. By introducing an additional parameter in the border constraints, the wind turbines are kept within a feasible distance to the turbines at the perimeter and in the neighboring subareas.

TOPFARM is able to optimize the complete wind farm in $m$ steps by including subareas. For each step, the turbines inside the active subarea are free to be relocated within the borders while the remaining turbines are fixed. The number of constraints is significantly reduced, since turbine distance constraints only need to be generated for turbines within the active subarea. The reduction in the number of constraints, $\text{Fixed}_1$, by including subareas, can therefore be rewritten as

$$\text{Fixed}_1 = T_f * s + T_f(T - T_f) + \frac{T_f(T_f - 1)}{2}. \tag{3.16}$$

The first part of the equation is related to reduction in border constraints, while the second and third part of the equation represent the reduction in turbine dis-

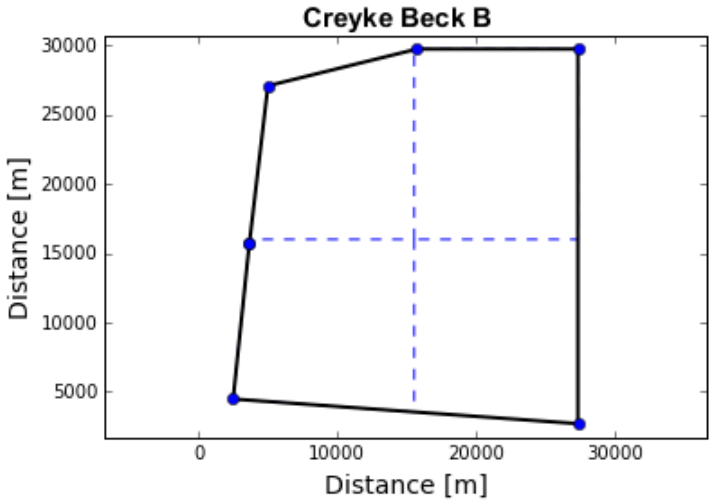


Figure 3.12: Subareas for Layout 1 and Layout 2.

tance constraints, which is significantly reduced compared to equation (3.13). By including the implementation of subareas in TOPFARM, the total number of constraints for Case 1, found by adding the equations (3.6), (3.11) and (3.16) together, can thus be rewritten as

$$\text{Const}_1 = (s - T_f)(T - T_f) + \frac{1}{2}(T(T-1) - T_f(T_f - 1)).$$

### 3.3.5 Increasing the quality of the AEP estimation

To obtain more accurate calculations of the power production during the optimization routine, a higher resolution regarding wind directions is necessary. Since the power production with respect to wind direction dimensions is highly nonlinear, the calculation of the AEP in TOPFARM is sensitive to this discretization. Ideally, the number of different wind directions considered in the calculation should be between 180 and 360. However, due to the high computational time, fewer directions must be considered in the optimization.

The goal of increasing the quality of the AEP calculation, is to help TOPFARM to make better decisions when optimizing the wind turbine layout. As an increase in resolution of the wind speed and wind directions when calculating the AEP, leads to a rapid increase in computational time for a large number of turbines, only

a subset of the wind turbines are evaluated in each step. By excluding some of the turbines from the optimization,TOPFARM is able to optimize the remaining layout with a higher AEP accuracy. The wind farm is thus divided into smaller subareas, where each subarea is optimized with the wake influence from only the neighboring subareas, as seen in Figure 3.13. This is justified by the fact that the wake from nearby turbines has a stronger influence than the wake from turbines further away.

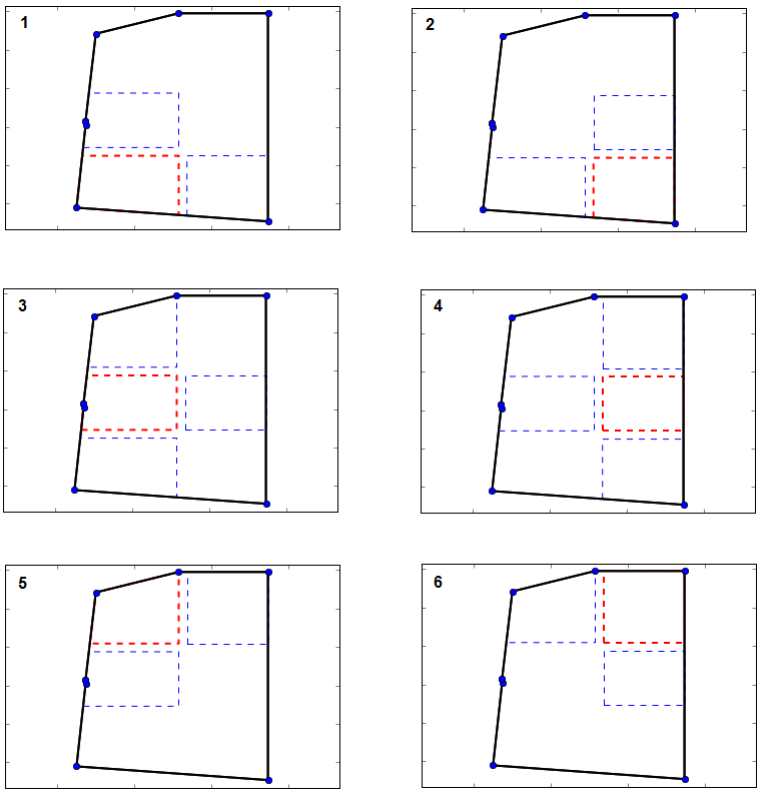


Figure 3.13: An illustration of the active (in red) and passive (in blue) subareas included in $m$ optimization steps.

# Chapter 4

# Experiments

## 4.1 Objective

The aim for this thesis is to find optimal layout suggestions for CBB, with the annual energy production as an objective. However, given the large costs related to offshore installation and operation, an increased production is not favorable at any cost. Even though the main focus in the generated experiments is to increase the AEP through optimization, the results obtained are also evaluated based on the profitability of the layouts.

## 4.2 Overview of experiments

The experiments generated in this thesis are developed for three different approaches on how to attain better layout suggestions for Creyke Beck B. The first approach is based on the assumption that TOPFARM is able to optimize initial layout suggestions with a significant AEP increase as a result. To test if the assumption holds, three initial layouts from Section 3.2.4 are used, where each layout is optimized with respect to various constraints. In total, nine unique experiments are conducted, where the relocation of turbines are allowed either within each column (column opt.), each row (row opt.) or each restricted area (free opt.) as shown in Table 4.1.

| | **Layout 1** | **Layout 2** | **Layout 3** |
|---|---|---|---|
| **Column Opt.** | Exp 1 | Exp 4 | Exp 7 |
| **Row Opt.** | Exp 2 | Exp 5 | Exp 8 |
| **Free Opt.** | Exp 3 | Exp 6 | Exp 9 |

Table 4.1: Overview of Experiments for Approach 1.

Motivated by the results obtained from the optimization in Creyke Beck B, the second approach evaluates the utilization of the available area. Here, the size of the wind farm is challenged by considering layouts distributed inside smaller areas. The aim of this approach is to achieve a reduction in costs, without generating a significant loss in AEP. Also, an increased improvement in production during the optimization procedure is expected for the denser layouts. To test these assumptions, the six initial layouts distributed inside areas ranging between 80% and 30% of the original wind farm from Section 3.2.4 are used. For each of these layouts, experiments are generated to further improve the attained production. As shown in the overview in Table 4.2, the experiments investigate whether the solution can be improved by performing a free optimization.

| | **CBB80** | **CBB70** | **CBB60** | **CBB50** | **CBB40** | **CBB30** |
|---|---|---|---|---|---|---|
| **Free Opt.** | Exp 10 | Exp 11 | Exp 12 | Exp 13 | Exp 14 | Exp 15 |

Table 4.2: Overview of Experiments for Approach 2.

The approach of improving the quality of the AEP calculation, is based on the assumption that a more detailed AEP calculation in the optimization process will contribute to better results. In order to evaluate this, two experiments are generated where the AEP is calculated based on a resolution of 21 wind speeds, and either 33 or 67 wind directions. The experiments are performed on the layout CBB40 using a free optimization, with a resolution of 33 directions in Exp 16 and 67 directions in Exp 17.

## 4.3 Results

### 4.3.1 Approach 1: Creyke Beck B layout optimization

The layouts inspired by Forewind (2013a) in Section 3.2.4 seem to be generated with respect to rules and regulations rather than attaining an optimal production. Therefore, performing an optimization on these layouts is triggered by the assumption that TOPFARM can provide better layout suggestions with a higher AEP, compared to the the production from the initial layouts given in Table 4.3. The aim is to reduce the wake losses given in Table 4.3, which denote the percentage of lost production of the theoretical maximum 5909935 MWh, from Section 2.2.4.

In order to evaluate this potential, three different optimization routines are performed on each layout. Two of these routines are designed to perform optimizations within each turbine column or turbine row. In this way, parts of the layout's original structure are maintained, while enabling an improvement in production. An advantage of this type of optimization, is that the program can run with a relatively low number of constraints compared to the size of the wind farm. The third optimization procedure is constructed to evaluate the potential of improvement, if the turbines are allowed to move freely within smaller subareas of the wind farm.

| | | **Layout 1** | **Layout 2** | **Layout 3** |
|---|---|---|---|---|
| **Dist perim** | [D] | 11.1 | 11.1 | - |
| **Dist col** | [D] | 13.5 | 10 | 13.8 |
| **Dist row** | [D] | 13.5 | 18 | 11.4 |
| **AEP** | [MWh] | 5445599 | 5446379 | 5411385 |
| **Wake loss** | [%] | 7.86 | 7.84 | 8.44 |

Table 4.3: Initial layout information for Layout 1, Layout 2 and Layout 3.

In total, nine experiments are conducted to evaluate the potential in AEP increase at Creyke Beck B. During the optimization procedure in each experiment, the calculation of the AEP is done by including the most frequently observed wind speeds $ws = [8, 10, 12]$, and wind directions $wd = [180, 210, 240, 270, 300, 330]$. The settlement of the wind conditions is derived from empirical evaluations of

the computational time and the final AEP increase obtained by various AEP resolutions. Triggered by the large turbine spacing shown in Table 4.3 between turbines on the perimeter (Dist perim), and in each row (Dist row) and column (Dist col), the minimum turbine spacing in the optimization is set to 10D, which is significantly larger than the suggested minimum of 6D. However, this adjustment has shown to be necessary, to help TOPFARM exploit the available area when relocating the turbines.

**Optimizing Layout 1**

Three experiments, Exp 1, Exp 2 and Exp 3 are constructed to perform layout optimizations on Creyke Beck B, with Layout 1 as initial input. In each experiment, the turbines on the perimeter are kept in their initial positions, while an optimization on the 72 wind turbines located inside the wind farm is performed. To limit the number of constraints, the full optimization procedure is run in several steps, dependent on the number of columns, rows or subareas. In Exp 1 and Exp 2, a total of nine steps are required as the wind farm consists of nine columns and rows. Exp 3 only requires four steps, as the free optimization divides the wind farm into four subareas. Due to the division of the subareas (see Section 3.3.4), the turbines within each subarea is set to relocate a distance of 7D away from the borders. This is done to maintain an acceptable distance from the turbines on the perimeter and inside the neighboring subareas.

Since an optimized layout might represent a local improvement rather than a global one, a complete wind farm optimization is run several times to investigate the presence of better solutions. In the experiments, a total of 10 optimization runs are thus performed. For each run, the optimal layout from the previous run is used as initial layout, to investigate new solutions. Figure 4.1 gives an overview of the AEPs obtained by the experiments in each run. The figure shows that two of the experiments Exp 2 and Exp 3, generate results with a lower production than the initial solution. It also shows that the change in production between each optimization run is relatively small, never more than 0.25 % from the initial production.

The best results from each experiment are presented in Table 4.4. Based on the number of constraints used to perform one optimization run, Table 4.4 shows

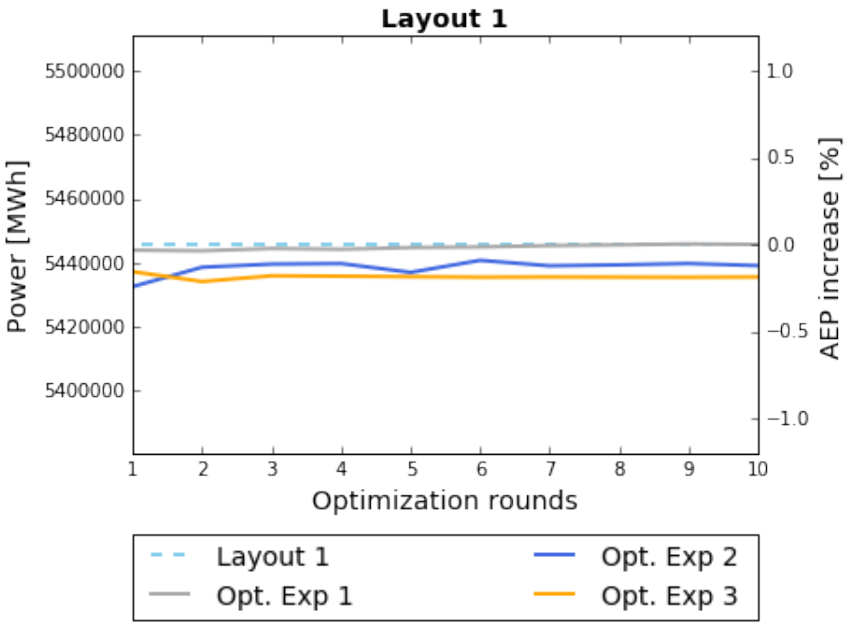


Figure 4.1: AEP values obtained during the optimization of Layout 1.

that Exp 3 might be more computationally demanding to optimize than the other experiments. However, the average calculated computational time for Exp 3 is only approximately 11 minutes longer.

| | | **Exp 1** | **Exp 2** | **Exp 3** |
|---|---|---|---|---|
| **Min dist** | [D] | 10 | 10 | 7 |
| **Constraints** | | 315 | 315 | 924 |
| **AEP Opt.** | [MWh] | 5445787 | 5440657 | 5437106 |
| **AEP Change** | [%] | 0.00 | -0.09 | -0.16 |
| **Wake loss** | [%] | 7.85 | 7.94 | 8.00 |
| **Avg. Time** | [min] | 44.67 | 44.42 | 56.24 |

Table 4.4: Optimization results for Layout 1.

When comparing the AEPs from the experiments to the initial productions in Table 4.3, none of the experiments show a reduction in wake loss. Instead, the experiments Exp 2 and Exp 3 even generate slightly bigger losses. Exp 1 is the only experiment with a non-negative AEP change, however the increase in production is so small, that it is not noticeable in the AEP change nor in the wake loss. Potential reasons for the observed deterioration in the experiments, will be discussed in

further detail in section 4.4.2.

A display of the optimal layouts generated byeach experiment is shown in Figure 4.2. The turbine distribution in the optimal layouts does not intuitively look like improved solutions, which is consistent with the results obtained in Table 4.4. The experiment with the least optimal solution namely Exp 3, also generate a layout which utilizes the total available area poorly. Even so, the decrease in production is relatively small compared to the amount of area which in Figure 4.2 (d) is empty. The lack of sensitivity regarding turbine placement is an interesting observation, which will be further examined in Section 4.4.2.

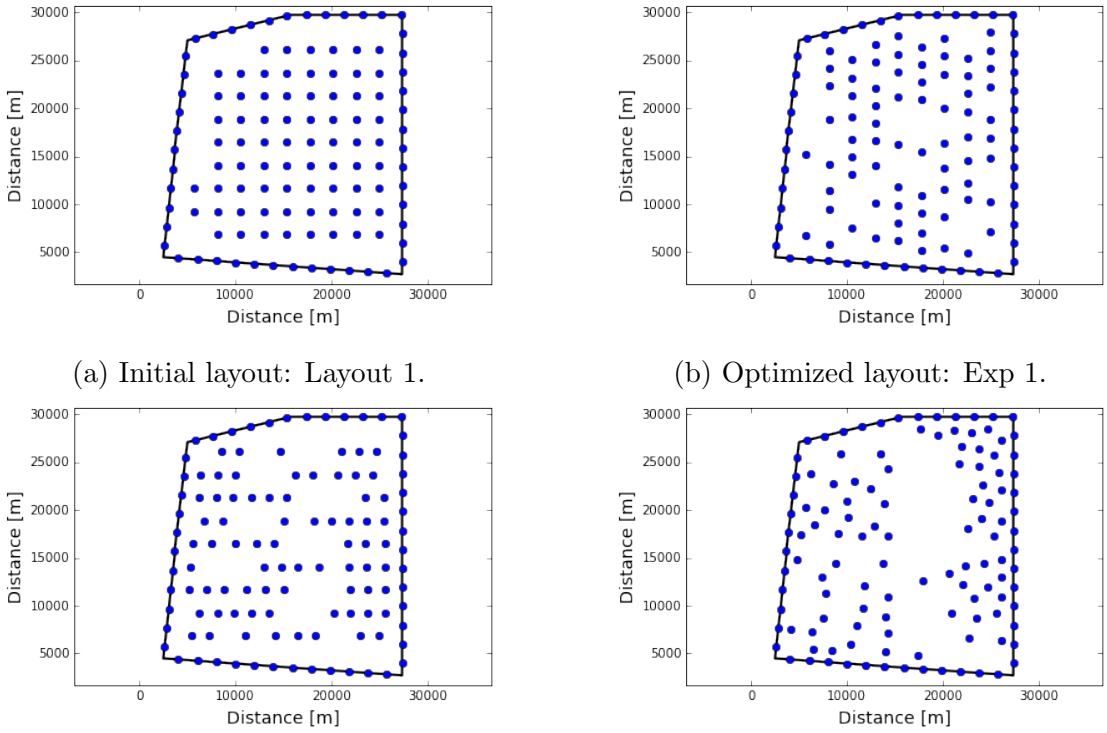


(a) Initial layout: Layout 1.

(b) Optimized layout: Exp 1.

(c) Optimized layout: Exp 2.

(d) Optimized layout: Exp 3.

Figure 4.2: Layout Results for Layout 1.

### Optimizing Layout 2

With the purpose of performing optimization runs on Layout 2, three experiments are constructed, namely Exp 4, Exp 5 and Exp 6. During the optimization, only the 72 turbines positioned inside the wind farm area are changed to better locations. A complete optimization of the wind farm is performed in six steps for Exp 4, and 13 steps in Exp 5, corresponding to the number of turbine rows and columns. Exp

6, which is divided into four subareas, only requires four steps to complete the optimization. As in Exp 3 for Layout 1, the turbines in Exp 6 are restricted to relocate a distance 7D away from the subarea borders.

All experiments, perform a total of 10 optimization runs to find an optimal layout, where the calculated production from every run is shown in Figure 4.3. From the figure, it becomes clear that only Exp 4 performs optimizations where the AEP value exceeds the initial production. The figure also shows that the change in AEP between each optimization run is relatively small, with a maximum change of 0.2 % from the initial production.

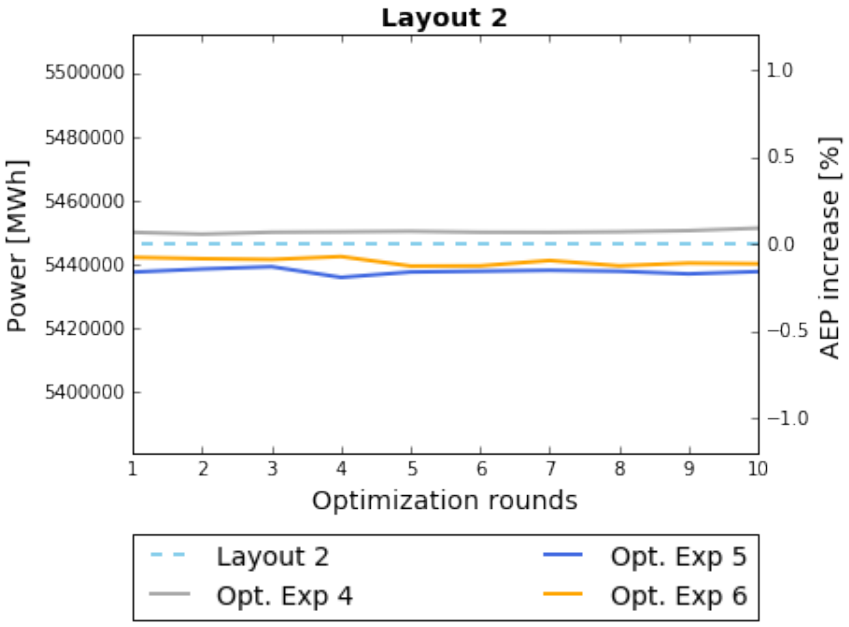


Figure 4.3: AEP values obtained during the optimization of Layout 2.

The best obtained results for each experiment are presented in Table 4.5. Due to the number of constraints and the average computational time, Exp 6 seems to be more demanding to optimize than the other experiments. In addition, it fails to attain an increase in AEP over the initial production from Layout 2. Only Exp 4 manage to achieve a small increase in production of approximately 0.09 %, which also generates a small decrease in wake loss. However, the change is too small to categorize the improvement as significant.

A display of the optimal layouts for each experiment is presented in Figure 4.4. The layout obtained by Exp 4 corresponds well with the AEP improvement observed,

| | | Exp 4 | Exp 5 | Exp 6 |
|---|---|---|---|---|
| **Min Dist** | [D] | 10 | 10 | 7 |
| **Constraints** | | 282 | 359 | 919 |
| **AEP Opt.** | [MWh] | 5451327 | 5439260 | 5442446 |
| **AEP Change** | [%] | 0.09 | -0.13 | -0.07 |
| **Wake loss** | [%] | 7.76 | 7.96 | 7.91 |
| **Avg. Time** | [min] | 41.92 | 47.07 | 76.42 |

Table 4.5: Optimization results for Layout 2.

as it appears to have a slightly larger turbine spacing in the columns compared to the initial layout. The layout distributions in both of Exp 5 and Exp 6, however seem to be less optimal than the initial solution, due to the several empty areas inside the wind farms. Although this is true, the decrease in production in both cases, is relatively small compared to their utilization of the available area.

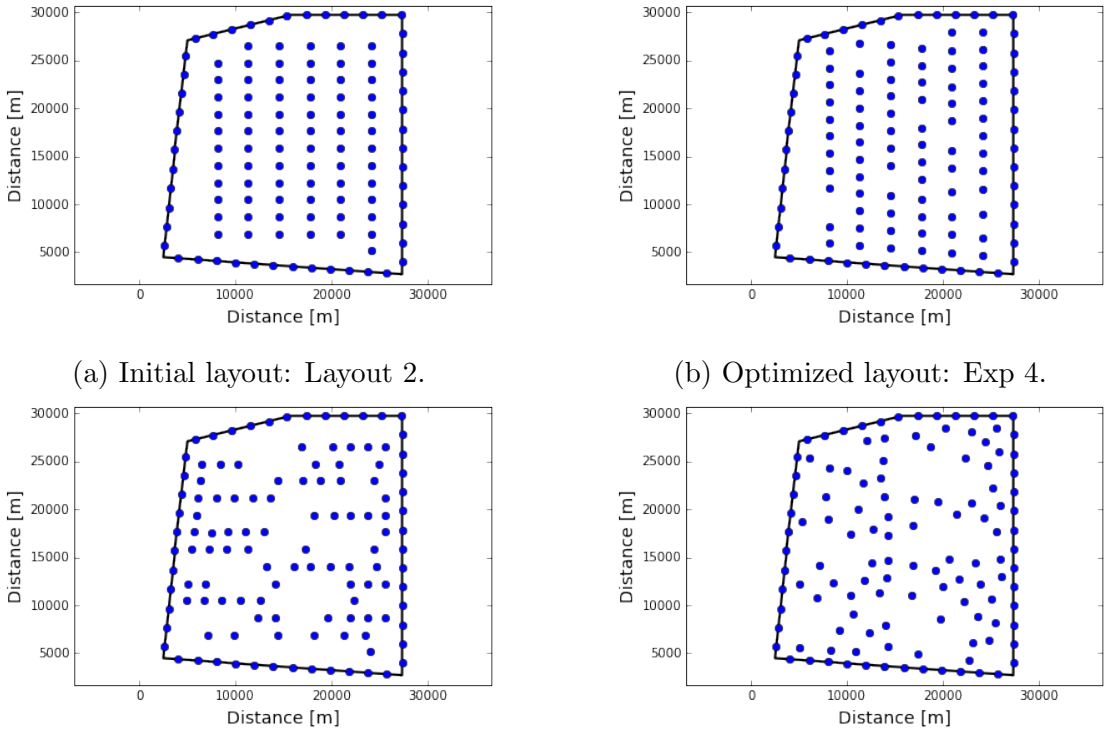


(a) Initial layout: Layout 2.

(b) Optimized layout: Exp 4.

(c) Optimized layout: Exp 5.

(d) Optimized layout: Exp 6.

Figure 4.4: Layout Results for Layout 2.

### Optimizing Layout 3

Three experiments, Exp 7, Exp 8 and Exp 9, are constructed to optimize Layout 3. In each experiment, all 120 turbines are relocated during a complete wind farm optimization. For Exp 7 and Exp 8, this is done during 10 and 12 steps, given by the number of turbine columns and rows. Experiment Exp 9 is divided into six subareas, and hence six steps are required for the complete optimization.

All experiments perform a total of 10 complete wind farm optimization runs, where the calculated production from each run is displayed in Figure 4.5. The figure shows that only experiment Exp 7 generate higher AEP values than the initial production. Even though the difference in the displayed productions is small for each optimization run, the variations are greater than for previously observed examples.

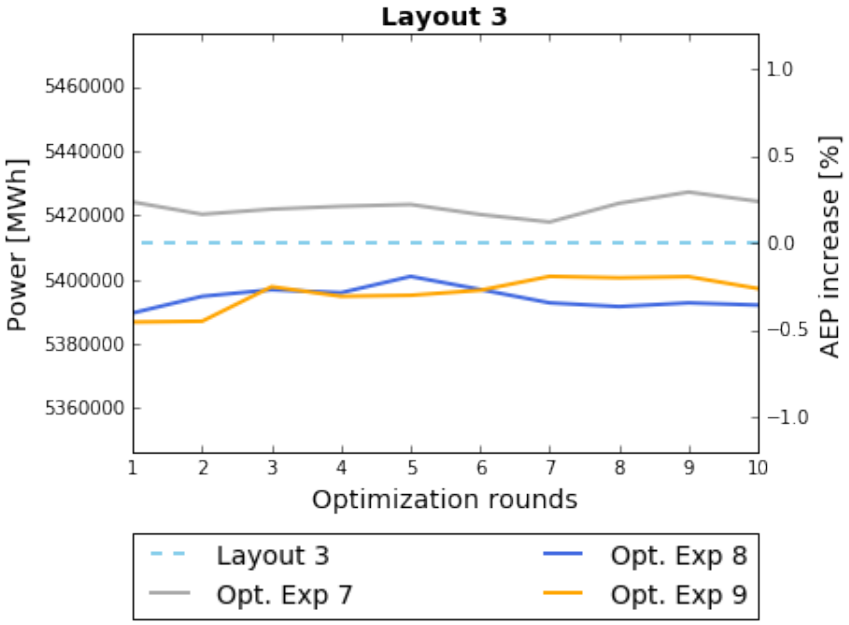


Figure 4.5: AEP values obtained during the optimization of Layout 3.

The best obtained results in each experiment are shown Table 4.6. Since all 120 turbines are included in the optimization procedure, more constraints are generated in the experiments for Layout 3, compared to the experiments for Layout 1 and Layout 2. Based on the number of constraints from Table 4.6, Exp 9 seems to be more computationally demanding than the other experiments. This observation is supported by the average calculated computational time, which on average is 50

minutes longer than in previous experiments.

The initial production from Table 4.3 is greater than the optimal production for both Exp 8 and Exp 9. However, Exp 7 manages to improve the AEP by 0.29 %. Even though this is better than what was achieved in the experiments for Layout 1 and Layout 2, the calculated wake loss is still higher.

| | | **Exp 7** | **Exp 8** | **Exp 9** |
|---|---|---|---|---|
| **Min Dist** | [D] | 10 | 10 | 10 |
| **Constraints** | | 470 | 492 | 1640 |
| **AEP Opt.** | [MWh] | 5427213 | 5400983 | 5400995 |
| **AEP Change** | [%] | 0.29 | -0.19 | -0.19 |
| **Wake loss** | [%] | 8.17 | 8.61 | 8.61 |
| **Avg. Time** | [min] | 72.32 | 69.19 | 121.59 |

Table 4.6: Optimization results for Layout 3.

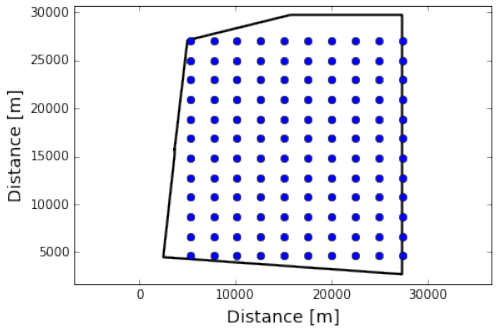


(a) Initial layout: Layout 3.

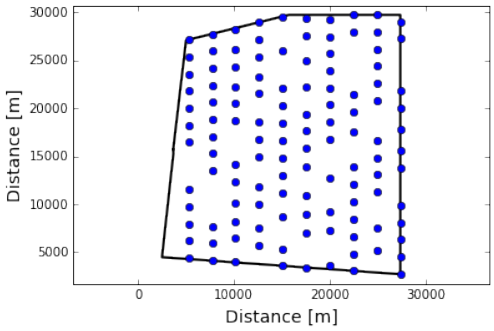


(b) Optimized layout: Exp 7.

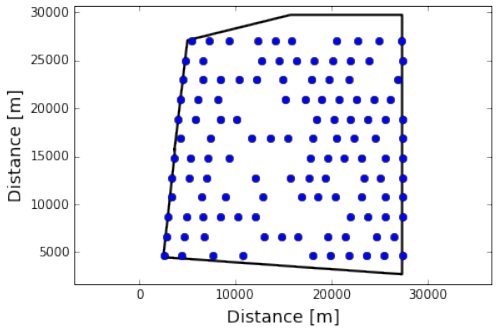


(c) Optimized layout: Exp 8.

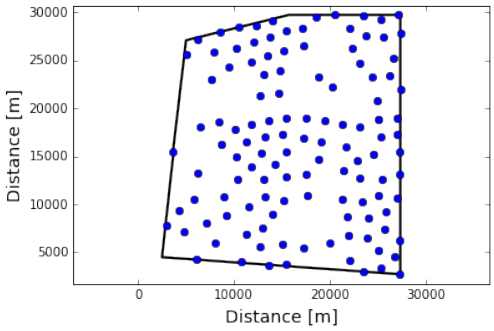


(d) Optimized layout: Exp 9.

Figure 4.6: Layout Results for Layout 3.

The display of the optimal layouts in Figure 4.6, provides a better understanding

of the results obtained in Table 4.6. As the available area in Layout 3 is not fully utilized, Exp 7 experiences a larger increase in production by exploiting the total area. For Exp 8 and Exp 9, the layout distribution consists of several empty areas within the wind farm, which might explain why the attained production is less than the initial production.

Common for all the experiments performed based on the three layouts, is that the column optimization provides increased AEPs, while the free optimization and the row optimization generate less optimal AEPs. Reasons behind this observation is discussed further in Section 4.4.1.

### 4.3.2 Approach 2: Wind farm area reduction

The main focus in the thesis is to attain maximum production, but not at any cost. Offshore, the high installation costs related to cables can for instance be significantly reduced, if the layout is distributed over a smaller area. The same applies to maintenance costs incurred in the operational phase. Thus, reducing the available area for turbine spacing can lead to a more profitable wind farm if the wake loss is not too high. To evaluate the change in production, a set of six initial layouts are constructed inside areas equivalent to 80%, 70%, 60%, 50%, 40% and 30% of the original Creyke Beck B area. The tables, Table 4.7 and Table 4.8 provide an overview of the initial layouts, including specifications such as initial production, area utilization and turbine spacing. The turbines inside each layout are organized into a number of columns and rows with turbine distances specified in the tables.

Figure 4.7 provides an overview of the production rate attained for the six initial layouts, compared to the utilized area. The production rate is given by the ratio between the attained AEP for each initial layout and the theoretical maximum of 5909935 MWh, from Section 2.2.4. As shown in Figure 4.7, the energy production is not very sensitive to the reduction in utilized area, motivating a further evaluation on this.

An experiment for each layout in Table 4.7 and Table 4.8 is made with the aim of attaining a reduction in the initial wake losses. In each experiment, an optimization

| | | CBB80 | CBB70 | CBB60 |
|---|---|---|---|---|
| **CBB ratio** | [%] | 80 | 70 | 60 |
| **Area** | [km$^2$] | 479.2 | 419.3 | 359.4 |
| **Colums** | | 10 | 10 | 8 |
| **Rows** | | 12 | 12 | 15 |
| **Dist col** | [D] | 11.16 | 10.44 | 9.68 |
| **Dist row** | [D] | 13.64 | 12.76 | 11.91 |
| **AEP** | [MWh] | 5405209 | 5374077 | 5338812 |
| **Wake loss** | [%] | 8.54 | 9.07 | 9.66 |

Table 4.7: Initial layout information for CBB80, CBB70 and CBB60.

| | | CBB50 | CBB40 | CBB30 |
|---|---|---|---|---|
| **CBB ratio** | [%] | 50 | 40 | 30 |
| **Area** | [km$^2$] | 299.5 | 239.6 | 179.7 |
| **Colums** | | 8 | 8 | 8 |
| **Rows** | | 15 | 15 | 15 |
| **Dist col** | [D] | 8.73 | 7.74 | 7.74 |
| **Dist row** | [D] | 10.55 | 9.94 | 7.46 |
| **AEP** | [MWh] | 5271146 | 5209079 | 5108093 |
| **Wake loss** | [%] | 10.81 | 11.86 | 13.57 |

Table 4.8: Initial layout information for CBB50, CBB40 and CBB30.

run is done by optimizing six separate subareas in which turbines are allowed to move freely. A total number of five optimization runs are performed during each experiment, where the best obtained results are presented in Table 4.9 and Table 4.10. The minimum distances presented in the tables, describe the minimum turbine spacing observed in the optimal solutions. Prior to the optimization, the minimum acceptable distance value is set between 8D and 6D in each experiment, depending on the area size.

The results from Table 4.9 and Table 4.10 show that the optimal solution for all experiments generate a wake loss which is greater than the loss from the initial layout. Hence, each experiment fail to produce better layouts. Compared to the

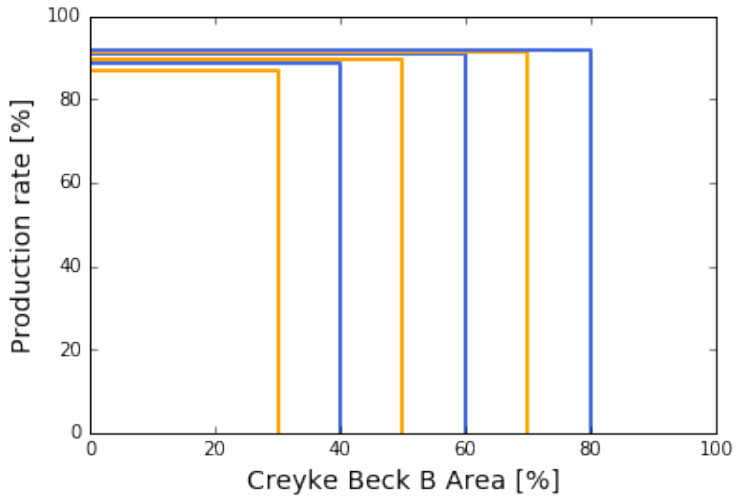


Figure 4.7: The production rate attained compared to the area reduction.

AEP change from earlier experiments, the results also indicate a greater negative change.

| | | Exp 10 | Exp 11 | Exp 12 |
|---|---|---|---|---|
| **CBB ratio** | [%] | 80 | 70 | 60 |
| **Min Dist** | [D] | 8 | 8.5 | 8 |
| **AEP Opt.** | [MWh] | 5366192 | 5325785 | 5297990 |
| **AEP Change** | [%] | -0.72 | -0.90 | -0.76 |
| **Wake loss** | [%] | 9.20 | 9.88 | 10.36 |
| **Avg. Time** | [min] | 130.28 | 125.85 | 163.17 |

Table 4.9: Optimization results for Exp 10, Exp 11 and Exp 12.

| | | Exp 13 | Exp 14 | Exp 15 |
|---|---|---|---|---|
| **CBB ratio** | [%] | 50 | 40 | 30 |
| **Min Dist** | [D] | 6 | 6 | 6 |
| **AEP Opt.** | [MWh] | 5235643 | 5147708 | 5058789 |
| **AEP Change** | [%] | -0.67 | -1.18 | -0.97 |
| **Wake loss** | [%] | 11.41 | 12.90 | 14.40 |
| **Avg. Time** | [min] | 153.47 | 149.07 | 148.08 |

Table 4.10: Optimization results for Exp 13, Exp 14 and Exp 15.

Some of the results from Table 4.9 and Table 4.10 are illustrated in more detail, to provide a better overview of the solutions. In Figure 4.8, the AEPs obtained in each optimization run for the experiments Exp 11, Exp 12 and Exp 13 are thus displayed. The figure shows that the optimized production in each experiment is consistently lower than the initial production. Another interesting result is that the optimal production attained in Exp 11 utilizing 70% of the available area, is lower than the initial production for Exp 12 utilizing 60% of the available area. This is also the case for the optimized production in Exp 10 compared to the initial production in Exp 11, which is notdisplayed in the figure.

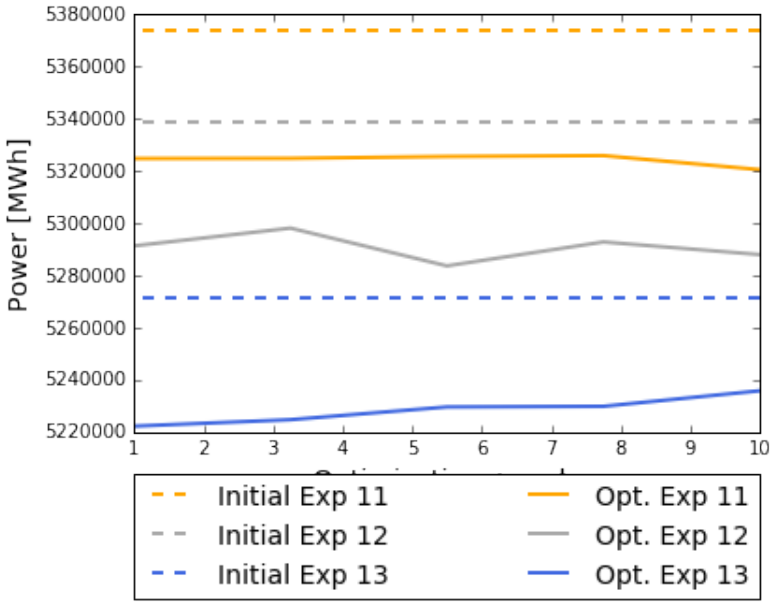


Figure 4.8: Initial and optimal AEP values for Exp 11, Exp 12 and Exp 13.

In addition to the obtained productions, the initial and optimal layouts for Exp 11, Exp 12 and Exp 13 are displayed in Figure 4.9. The figure gives an accurate representation of the area reduction, compared to the outline of Creyke Beck B. An observation from Figure 4.9 is that the turbines are not as uniformly distributed in the optimal layouts. Several open areas can also indicate that the full potential inside the reduced wind farms is not exploited.

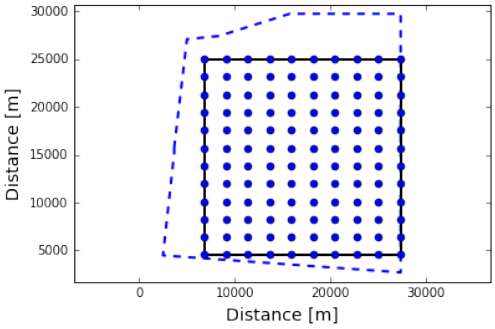


(a) Initial layout: CBB70.

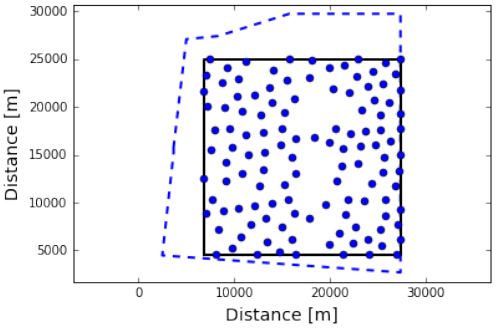


(b) Optimized layout: Exp 11.

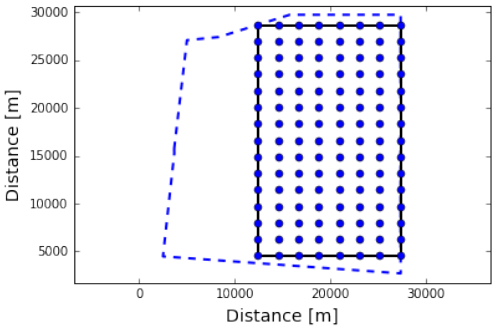


(c) Initial layout: CBB60.

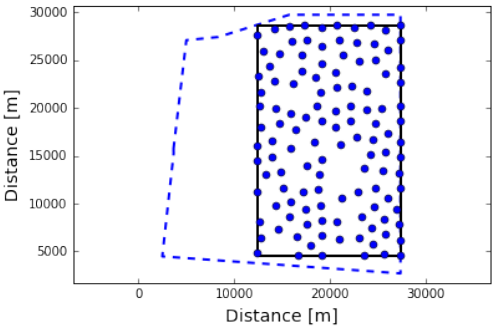


(d) Optimized layout: Exp 12.

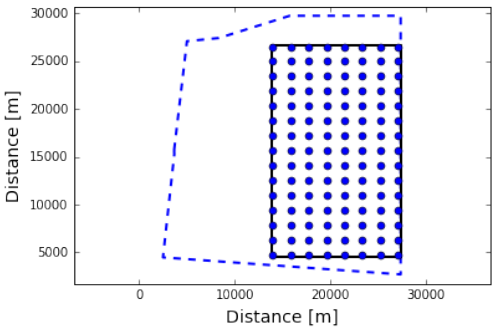


(e) Initial layout: CBB50.

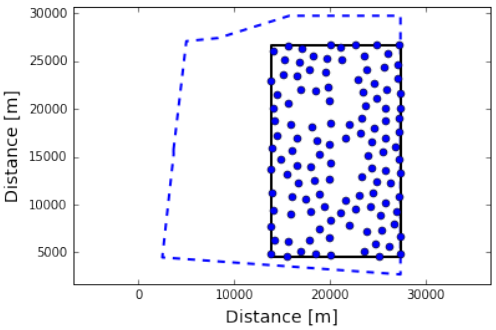


(f) Optimized layout: Exp 13.

Figure 4.9: Initial and Optimal layouts for the experiments Exp 11, Exp 12 and Exp 13.

### 4.3.3 Approach 3: Increasing the resolution

So far, most of the experiments have produced negative results during the optimization. Even though reducing the area and hence the turbine spacing provided some interesting results in the previous section, an increase during the optimization routines was not achieved. Therefore, a third approach to improving the optimized solutions is investigated.

The previous experiments are constructed to calculate the initial and optimal AEPs with a high resolution of 21 wind speeds and 180 wind directions, and the AEPs during the optimization routine with a low resolution of 3 wind speeds and 6 directions, respectively. Due to the high variation in resolution, layouts evaluated as improved solutions by the calculated AEP in the optimization procedure, can end up being less optimal when AEP calculations of higher quality are performed. To determine the sensitivity of the AEP calculations, the effect of changing the resolution of the wind speeds and wind directions is evaluated, with the results displayed in Figure 4.10 and Figure 4.11.

Figure 4.10 shows the variations in attained AEP in Layout 3, for different resolutions of the wind direction. The calculations are performed for three different choices of wind speed resolutions, where either 6, 12 or 21 discrete wind speeds are included in the calculation.

The results obtained in Figure 4.10 show an overall increase in production when increasing the wind direction resolution. In the range between 6 and 179 included wind directions, the attained AEP is increased with approximately 37 %. Thus, the variation in calculated AEP in the optimization procedure, compared to the initial and optimal AEP calculations, is significant. It is also observed that the variations in attained AEP with respect to the chosen wind speed resolution is small, where choosing resolutions of 12 and 21 wind speeds result in nearly identical AEP estimations.

To determine if the graphical shape in Figure 4.10 is consistent for various wind directions, several AEP calculations with the same wind direction resolution, but with different wind direction discretizations, are performed. This is done by changing the range of the wind directions from 0 degrees and 360 degrees, to $0+n$ degrees

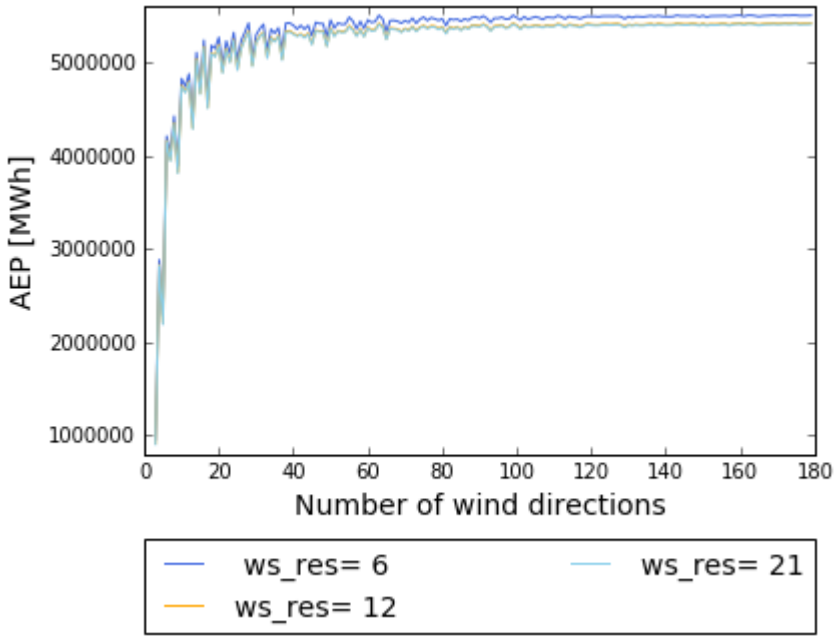


Figure 4.10: Change in calculated AEP with increasing resolution for the wind direction for Layout 3, for three wind speed resolutions.

and $360+n$ degrees respectively, since $0+n$ and $360+n$ denote the same direction for an arbitrarily chosen $n$. In addition to the original starting direction at 0 degrees used in Figure 4.10, ranges starting from $n = 15$, $n = 30$, $n = 45$, $n = 60$ and $n = 75$ degrees are also included, to attain different wind direction discretizations. Figure 4.11 gives an overview of the obtained results, where AEPs are calculated for 2 to 40 wind directions, which from Figure 4.10 is the number of directions generating a significant change in attained AEP.

Based on Figure 4.11, the overall increase in production by including more directions seems to be consistent for different discretizations of the wind direction. Since the calculated AEP appear to be significantly influenced by the choice of wind directions, it is assumed that by increasing the AEP resolution in the optimization procedure, improved optimal solutions may be attained, thus motivating the approach of increasing the AEP resolution.

In Figure 4.10, the AEP starts to converge when including resolutions between 40 and 60 wind directions. Thus, the approach on increasing the quality of the AEP calculation aim to include approximately 60 wind directions in the optimization procedure. Due to the increased computational time related to high resolution

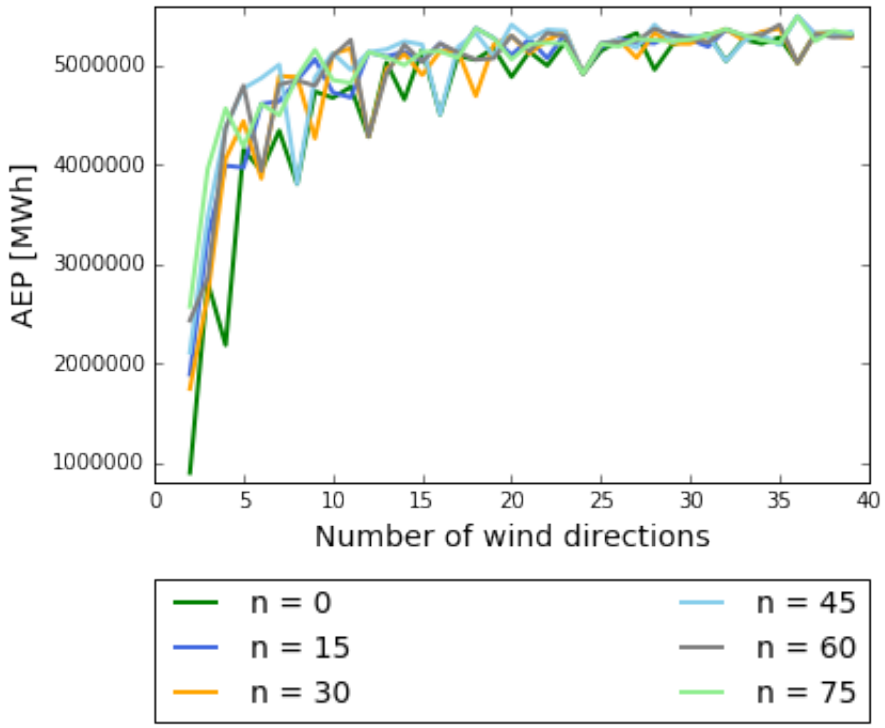


Figure 4.11: Change in calculated AEP with increasing resolution of the wind direction for Layout 3, for different wind discretizations.

AEP calculations, the implementation in Section 3.3.5 is included in the optimization, to enable sufficiently high AEP resolution calculations. In total, two experiments, Exp 16 and Exp 17, are constructed to investigate whether the solution can be improved. The experiments are performed on the reduced layout CBB40, where six separate subareas are optimized by relocating the turbines within each subarea freely. In the two experiments Exp16 and Exp17, the AEP resolution inside the optimization procedure is set to 33 and 67 wind directions, respectively. The results for each experiment are presented in Table 4.11, which also includes the results from Exp 14.

Despite the extreme AEP variations observed by including different numbers of wind directions, the improvement attained by increasing the AEP resolution in the optimization is very low. The results indicate that an increase in number of wind directions included in the optimization improves the optimal AEP. However, the obtained AEPs for both Exp 16 and Exp 17 are still less than the initial production. In addition, the small improvement in production compared to Exp 14, comes at a high cost in terms of computational time. While Exp 14 on average

| | | Exp 14 | Exp 16 | Exp 17 |
|---|---|---|---|---|
| **CBB Ratio** | [%] | 40 | 40 | 40 |
| **Wind dir.** | | 6 | 33 | 67 |
| **AEP Opt.** | [MWh] | 5147708 | 5163901 | 5194033 |
| **AEP Change** | [%] | -1.18 | -0.87 | -0.29 |
| **Wake loss** | [%] | 12.90 | 12.62 | 12.11 |
| **Avg. Time** | [min] | 149 | 2142.8 | 3485.7 |

Table 4.11: Optimization results for Exp 16 and Exp 17, compared to Exp 14.

runs an optimization round in approximately 2.48 hours, Exp 16 and Exp 17 spend 35 and 58 hours, respectively. Based on the low rate of improvement compared to the large increase in computational time, there is little point in increasing the AEP resolution further.

## 4.4 Discussion

A common feature of all the experiments, is that they do not manage to generate layout suggestions resulting in a significant increase in AEP. In most experiments, the optimized production is even lower than the production calculated for the initial solution. The fact that the experiments fail to generate optimal solutions of significance, is a setback for the scope of the thesis. Even so, a further discussion on topics related to the optimization routines and their performance is relevant, to identify areas with a potential of improvement. Despite the generation of negative results, some interesting discoveries are also achieved, which should be relevant for further investigations. A discussion on various topics related to identifying problems or determining interesting results is thus provided in this section.

### 4.4.1 Optimization within each column, row or sub area

When optimizing the three initial layouts for Creyke Beck B in experiment Exp 1 to Exp 9, three different optimizations, which either relocate the turbines within each

column, row or subarea are run. While the experiments performing an optimization within each column manage to provide a small increase in AEP, the experiments optimizing within each row or subarea consistently generate AEP values lower than the initial production. To better understand why these approaches return different results, a further discussion on the topic is provided.

Apart from the direction in which the turbines are allowed to be relocated, the structure of the optimization within each column and row is nearly identical. Therefore it is likely that the variation in results is caused by the estimation of wakes inside the AEP calculation during the optimization. One possibility, is that the simplified wake field generated in the optimization due to a low resolution of wind speeds and wind directions, represents the most influencing wakes with respect to a relocation of turbines inside each column rather than rows. If this is the case, an improvement in results when optimizing turbine rows can be attained, by changing the discretization of the wind directions included in the AEP calculation. Another explanation may be that the potential for improvement is greater when optimizing the columns rather than the rows. When examining the wind rose for Creyke Beck B in Figure 2.7, the most frequently observed winds are west-southwesterly, which also indicate dominant wake lines in these directions. Therefore, relocating turbines in the north-south directions is likely to be more efficient for minimizing the wake effect and hence maximizing the AEP, than relocating turbines in the direction of the mean wake field, from east to west.

Since the turbine relocation within smaller subareas introduces a larger variety in turbine distribution compared to the row and column optimization, the solutions generated by this routine are expected to attain the highest AEPs. Instead, the results show a production which is less optimal than the initial solution. Hence, it seems like the optimization procedure fail to take advantage of the opportunity to relocate turbines more freely. Considering the size of the problem, an explanation can be that TOPFARM is not capable of handling the large amount of design variables, despite the included implementations.

### 4.4.2 TOPFARM performance

Based on the results from the experiments, two main observations are made on TOPFARM's performance. The first observation is that the experiments usually fail to generate solutions which exceed the initial production. The second observation is that the AEP change between the initial and the optimal production is small, even for diverse layouts. To understand why TOPFARM fails to perform as expected, plausible reasons behind these results are discussed, like the potential of improvement and program limitations.

#### Potential of improvement

Given the small changes between the optimal and the initial AEP calculations obtained in the experiments, it is natural to investigate the potential for attaining improved solutions. If the initial layouts already represent optimal solutions, performing optimizations on them becomes excessive. One way of determining the potential of improvement, is to evaluate the effect from the wake field on downstream turbines. If the wake field dissipates before reaching other turbines, there is no need to improve the initial layout with respect to the AEP. For the initial and the optimal layouts from Exp 1 to Exp 9, the loss in production is estimated to be approximately 8 %, thus theoretically, there exist a potential in improving the solutions. In practice however, this potential is dependent on the wake contributions on the wind field. If the generated wind field including contributions from wakes is uniform, diverse layouts are more likely to attain almost equal AEPs, thus reducing the probability of attaining better layout suggestions. The attained AEP values from Exp 1 to Exp 9 are all close to the initial production, even though the corresponding layouts are quite diverse. These observations strengthen the assumption of a uniform wind field for layouts utilizing the available Creyke Beck B area. Thus based on these observations, it is possible that Layout 1 and Layout 2 represent near optimal solutions with respect to attaining maximal AEP.

The production rates attained for the initial layouts on the reduced Creyke Beck B areas in Figure 4.7, support the theory of a uniform wind field, as the reduction in production rates is significantly smaller than the reduction in area. However, when performing optimizations on these layouts, the optimal solutions are even

further away from the initial production. Since a uniform wind field does not justify the generation of less optimal results, it is evident that there must exist other components influencing the results.

### Program limitations

A challenging task throughout the thesis, has been to run TOPFARM for sufficiently large test cases. Even though the added implementations enable TOPFARM to perform optimizations on various problems, there is still a possibility that the program's performance is inhibited by the size of the problem. As several of the components which TOPFARM is based on are accepted as unknown (black boxes) in the thesis, there is some degree of uncertainty in how introduction of larger test cases will be impacted. As a result, identifying the components resulting in less optimal solutions can be challenging. Even so, it is possible to point to several components as particularly interesting for further investigations, like the choice of optimizer and the AEP estimation.

The choice of optimizer is an important element in the optimization procedure, which may have a significant influence on the results. Several different optimizers are available in the TOPFARM library, including the chosen optimizer for the experiments, COBYLA. The decision of using COBYLA as an optimizer, is based on observations from available TOPFARM tutorials, and recommendations from the developers. Still, without empirical evaluations, COBYLA's performance compared to the other optimizers, remain uncertain. Therefore, there is a possibility that improved solutions can be attained, by including a different optimizer.

In addition to the optimizer, the calculation of the AEP is a key element in the optimization, which directly influences the results. Since the AEP calculations inside the optimization procedure are less accurate than the initial and optimal AEP calculations, this may enable less optimal results to be generated. Therefore, evaluating the AEP resolution has been a focus area in the thesis, where increasing the resolution in the optimization has been investigated in hopes of attaining improved solutions. Even though the results from the approach fail to attain improved solutions when increasing the resolution, some interesting observations are still made.

Firstly, Figure 4.10 shows that the calculated AEP is highly dependent on the resolution of the wind directions, especially for low resolutions. As a result, the calculated AEP including six wind directions in the optimization procedure, becomes a poor representation of the actual production. This observation strengthens the assumption that less optimal results are allowed due to the calculation of the AEP. Secondly, the rapid monotonic increase observed in Figure 4.11 for different discretizations of the wind directions, is unexpected. Intuitively, it is assumed that by plotting the attained AEP calculations for different numbers of directions, a fluctuating curve converging to an equilibrium is attained. Even though the plots in Figure 4.10 and Figure 4.11 contain fluctuations, they show an overall monotonic increase in AEP, converging to a maximum, when increasing the wind direction resolution.

Based on these observations, it is considered relevant to do a thorough evaluation of the AEP calculation, to understand why this increase is observed, and to control that there are no bugs inside the code. Also, there are reason to believe that the AEP calculations may contribute to the generation of less optimal results in several of the experiments. Considering that the AEP calculation of improved accuracy does not result in improved solutions, while the computational time is significantly increased, it is also relevant to consider different AEP calculation methods or including a different wake model for large test cases like Creyke Beck B.

### 4.4.3 Area utilization

By reducing the available area in which turbines can be located, costs related to installation and operation of the wind farm can be significantly reduced. However, such reductions also comes with a price of less attained AEP, due to a tighter turbine spacing. Therefore, in order to determine the best utilization of a given area, the loss in attained AEP must be compared to the potential cost savings, for the various layouts.

From Figure 4.7 it is apparent that generating layouts inside significantly smaller areas by reducing the turbine spacing, results in a relatively small production loss. Therefore, utilizing only a fraction of the available Creyke Beck B area can

potentially result in large cost savings. Still, since the AEP is the only economical income, a small decrease in production can cause large economical losses during the wind farms operational lifetime. Thus a thorough evaluation on overall costs is required, to determine if reducing the utilized area results in a decrease in the LCoE. It is beyond the scope of this thesis to assess the potential cost savings, as this requires an excessive amount of work. Still, the results obtained in Figure 4.7 indicate a promising potential, which is relevant to investigate further. If confirmed as a cost reducing factor, utilizing a smaller area of Creyke Beck B could increase the revenue of the wind farm, and become valuable input to Forwind's wind farm planning.

# Chapter 5

# Summary and Outlook

## 5.1 Summary

The scope of the thesis has been to find optimal layouts with the annual energy production as an objective, for the planned offshore wind farm Creyke Beck B. In order to improve the various initial layouts, the powerful wind farm optimization tool, TOPFARM, has thus been applied. In addition, wind data from Nora10 and turbine data from DTU's 10MW reference wind turbine have been included, to provide a good description of the wind resource and power estimate at Creyke Beck B.

Since TOPFARM is originally designed to handle smaller test cases, a great amount of time has been spent on the process of enabling optimizations of large wind farms. During this process, three main challenges have been identified, namely enabling TOPFARM to handle the required amount of turbines, performing optimizations where the specified constraints are upheld, and increasing the velocity and wind speed resolution for the AEP calculations in the optimization procedure. To meet these challenges, various implementations have been constructed, where the implementations of fixating turbines and constructing wind farm subareas, have been a crucial factor for enabling the required number of turbines in the optimization. In addition, the border constraints and wind turbine distance constraints have been implemented to guarantee a feasible relocation of turbines, while AEP calculations including a higher resolution of the velocity and the wind directions have

been implemented to enable optimizations based on AEP calculations of improved accuracy.

In total, three approaches to obtain optimal layouts in Creyke Beck B have been attempted. The first approach, evaluating three sets of rules for turbine relocation on three initial layouts, has returned results which overall show small improvements compared to the initial suggestions. From the second approach on evaluating the utilization of the available area, a potential in cost savings related to installation and operation of the wind farm has been discovered. The third approach has been made to improve the solutions from the second approach, but has returned unsatisfying results.

Based on the results from the experiments and the following discussion, some concluding remarks from the thesis can be made. For instance, it is observed that relocating turbines when utilizing the total Creyke Beck B area, has little effect on the calculated AEP. Considering the low potential for generating improved solutions, Layout 1 and Layout 2 might represent near optimal solutions with respect to attaining maximal AEP. Still, utilizing the total available area might not be optimal with respect to the LCoE. Considering the relatively small production losses compared to the reduction in utilized area, it is a possibility that large cost reductions can be achieved, by restricting the turbines within a fraction of the Creyke Beck B area. However, a further analysis of improved solutions and LCoE evaluations is required, to determine if reducing the area is an optimal solution.

Since several of the obtained results from the optimization procedure generate lower AEP values than the initial solution, it is apparent that the current version of TOPFARM struggle to attain optimal solutions for the given problem. Considering that TOPFARM is designed to handle smaller test cases, it is reasonable to think that the lack of improvement in the results is related to the size of the wind farm with respect to the number of turbines. Without validation from testing, the obstacles preventing the generation of improved results remain undetermined. Even so, the discussion in Section 4.4.2 provides reasonable suggestions for changes that could contribute towards improved solutions, like an extensive research on the choice of optimizer and how the AEP is estimated.

## 5.2 Outlook

Based on the unexpected and rapid increase in calculated AEP when increasing the resolution of the wind speeds and wind directions, a quality check of the AEP estimations in TOPFARM is suggested. For large wind farms, attaining fast but sufficiently accurate wind field estimates, are crucial for both the AEP predictions and the optimization. Thus, useful future work can be to test alternative wake models, like the Jensen model or Fuga. In addition, a further analysis of various optimizers is proposed, as this may lead to improved results when applying TOPFARM on large test cases. Thus, evaluating the performance of the available optimizers through empirical research, and possibly implementing additional optimizers in TOPFARM, are considered relevant.

The profitability of a large wind farm project like Creyke Beck B, is highly dependent on minimizing the LCoE, where various cost components need to be evaluated. Therefore, a further expansion of the model is suggested, to evaluate costs in addition to the attained production. An interesting problem in particular, can be to include electrical grid costs in the objective. By doing so, large turbine distances, which may be optimal with respect to attaining maximum AEP, also introduce an increase in cable costs. This is a highly relevant topic in wind farm optimization in general, but can be especially interesting for Creyke Beck B to further evaluate the optimal utilization of the available area.

# Bibliography


4C Offshore (2013). 4C Global Offshore Wind Farms Database. URL: http://www.4coffshore.com/offshorewind/. Last accessed on May.18.2016.

Arent, D., Sullivan, P., Heimiller, D., Lopez, A., Eurek, K., Badger, J., Jørgensen, H. E., Kelly, M., Clarke, L., and Luckow, P. (2012). Improved Offshore Wind Resource Assessment in Global Climate Stabilization Scenarios. Technical Report NREL/TP-6A20-55049.

Bak, C., Zahle, F., Bitsche, R., Kim, T., Yde, A., Henriksen, L. C., Natarajan, A., and Hansen, M. H. (2013). Description of the DTU 10 MW Reference Wind Turbine. Technical Report DTU Wind Energy Report-I-0092, DTU Wind Energy, Roskilde.

Barthelmie, R. J., Hansen, K., Frandsen, S. T., Rathmann, O., Schepers, J. G., Schlez, W., Phillips, J., Rados, K., Zervos, A., Politis, E. S., and Chaviaropoulos, P. K. (2009). Modelling and Measuring Flow and Wind Turbine Wakes in Large Wind Farms Offshore. *Wind Energy*, 12(5):431–444.

Department of Energy and Climate Change (DECC) (2011). Renewable Energy Roadmap Update 2012. Technical report, London.

DTU Wind Energy (2015). Wake model for offshore wind farms. URL: http://www.wasp.dk/fuga. Last accessed on May.7.2016.

DTU Wind Energy (2016). Wind resources for energy production of wind turbines. URL: http://www.wasp.dk/wasp. Last accessed on May.3.2016.

Ehrlich, R. (2013). *Renewable energy: a first course*. CRC Press, Boca Raton.

Ernst and Young (EY) (2015). Offshore wind in Europe: Walking the tightrope to success. Technical report.

Forewind (2012). Dogger Bank Zone.
URL: http://www.forewind.co.uk/news/60/15/Forewind-announces-first-four-Dogger-Bank-project-boundaries.html. Last accessed on May.23.2016.

Forewind (2013a). Dogger Bank Creyke Beck: Environmental Statement Chapter 5 Project Description. Technical Report F-OFC-CH-005.

Forewind (2013b). Dogger Bank Teesside A & B: Draft Environmental Statement Chapter 5 Project Description. Technical Report F-OFL-CH-005.

Forewind (2016). Development process. URL: http://www.forewind.co.uk/zone-development/zone-development-overview.html. Last accessed on May.13.2016.

Hau, E. (2006). *Wind turbines: Fundamentals, Technologies, Application, Economics*. Springer, Berlin, 2nd edition.

Haugland, J. K. and Haugland, D. (2012). Computing the Optimal Layout of a Wind Farm. *NIK-2012 Conference*, pages 93–104.

Heggelund, Y., Jarvis, C., and Khalil, M. (2015). A fast reduced order method for assessment of wind farm layouts. *Energy Procedia*, 80:30–37.

Herbert-Acero, J. F., Probst, O., Réthoré, P. E., Larsen, G. C., and Castillo-Villar, K. K. (2014). A Review of Methodological Approaches for the Design and Optimization of Wind Farms. *Energies*, 7(11):6930–7016.

Jensen, N. O. (1983). *A note on wind generator interaction*. Risø National Laboratory, Roskilde.

Katić, I., Højstrup, J., and Jensen, N. O. (1986). A simple model for cluster efficiency. In *European Wind Energy Association Conference and Exhibition*, pages 407–410, Rome.

Larsen, G. C. (1988). *A simple wake calculation procedure*. Risø National Laboratory, Roskilde.

Larsen, G. C. (2009). A simple stationary semi-analytical wake model. Technical Report Risø-R-1713(EN), Risø DTU, Roskilde.

Larsen, G. C., Aagaard Madsen, H., Troldborg, N., Larsen, T. J., Réthoré, P.-E., Fuglsang, P., Ott, S., Mann, J., Buhl, T., Nielsen, M., Markou, H., Sørensen,

J. N., Hansen, K. S., Mikkelsen, R. F., Okulov, V., Shen, W. Z., Heath, M., King, J., McCann, G., Schlez, W., Carlén, I., Ganander, H., Migoya, E., Crespo, A., Jiménez, A., Prieto, J. L., Stidworthy, A., Carruthers, D., Hunt, J., Gray, S., Veldkamp, D., Mouritzen, A. S., Jensen, L., Krogh, T., Schmidt, B., Argyriadis, K., and Frohböse, P. (2011). TOPFARM - next generation design tool for optimisation of wind farm topology and operation. Technical Report Risø-R-1805(EN), Danmarks Tekniske Universitet, Risø Nationallaboratoriet for Bæredygtig Energi.

Larsen, G. C. and Réthoré, P.-E. (2013). TOPFARM – A Tool for Wind Farm Optimization. *Energy Procedia*, 35:317–324.

Løland, L. (2015). Analysis of Grid-Connected Wind Farm Combined With Hydrogen Production. Master's thesis, Norwegian University of Life Sciences.

NationMaster (2011). United Kingdom Energy Stats. URL: http://www.nationmaster.com/country-info/profiles/United-Kingdom/Energy. Last accessed on May.13.2016.

Okulov, V. L. and Sørensen, J. N. (2008). Refined Betz limit for rotors with a finite number of blades. *Wind Energy*, 11(4):415–426.

Ott, S., Berg, J., and Nielsen, M. (2011). Linearised CFD Models for Wakes. Technical Report Risø-R-1772(EN), Risø National Laboratory, Roskilde.

Perez, R. E., Jansen, P. W., and Martins, J. R. R. A. (2012). pyOpt: a Python-based object-oriented framework for nonlinear constrained optimization. *Structural and Multidisciplinary Optimization*, 45(1):101–118.

Powell, M. J. D. (1994). A direct search optimization method that models the objective and constraint functions by linear interpolation. In *Advances in optimization and numerical analysis*, pages 51–67. Springer Netherlands.

Reistad, M., Breivik, O., and Haakenstad, H. (2007). A high-resolution hindcast study for the north sea, the norwegian sea and the barents sea. *Proceedings of the 10th International Workshop on Wave Hindcast and Forcasting and Coastal Hazard Symposium*.

Renkema, D. J. (2007). Validation of wind turbine wake models. Master's thesis, Delft University of Technology.

Réthoré, P. E., Fuglsang, P., Larsen, G. C., Buhl, T., Larsen, T. J., and Madsen, H. A. (2014). TOPFARM: Multi-fidelity optimization of wind farms. *Wind Energy*, 17(12):1797–1816.

Van Bussel, G. J. W. and Zaayer, M. B. (2001). Reliability, Availability and Maintenance aspects of large-scale offshore wind farms, a concepts study. In *MAREC 2011: Proceedings of the 2-day International Conference on Marine Renewable Energies, Newcastle, UK, 27-28 March 2001*. Institute of marine engineers.

Wallace, J. M. and Hobbs, P. V. (2006). *Atmospheric Science: an introductory survey*. Academic press, London, 2 edition.